AD NUMBER

AD462877

NEW LIMITATION CHANGE

TO

Approved for public release, distribution unlimited

FROM

Distribution authorized to U.S. Gov't. agencies and their contractors; Administrative/Operational Use; Mar 1965. Other requests shall be referred to Air Force Avionics Lab., Research and Technology Div., Wright-Patterson AFB, OH 45433.

AUTHORITY

ASD ltr dtd 8 Dec 1970

UNCLASSIFIED

AD 462877

DEFENSE DOCUMENTATION CENTER

FOR

SCIENTIFIC AND TECHNICAL INFORMATION

CAMERON STATION ALEXANDRIA, VIRGINIA

UNCLASSIFIED

SOME ASPECTS OF THE TANGENT-ANGLE VS. ARC LENGTH REPRESENTATION OF CONTOURS

Juris G. Raudseps
Communication and Control Systems Laboratory

The Ohio State University
Research Foundation
Columbus, Ohio

TECHNICAL REPORT 1801-6

March 1965

Contract AF 33(615)-1267

Project No. 414408

Task No. 4144

Air Force Avionics Laboratory
Research and Technology Division
Air Force Systems Command
United States Air Force
Wright-Patterson Air Force Base, Ohio

NOTICES

When Government drawings, specifications, or other data are used for any purpose other than in connection with a definitely related Government procurement operation, the United States Government thereby incurs no responsibility nor any obligation whatsoever, and the fact that the Government may have formulated, furnished, or in any way supplied the said drawings, specifications, or other data, is not to be regarded by implication or otherwise as in any manner licensing the holder to any other person or corporation, or conveying any rights or permission to manufacture, use, or sell any patented invention that may in any way be related thereto.

The Government has the right to reproduce, use, and distribute this report for governmental purposes in accordance with the contract under which the report was produced. To protect the proprietary interests of the contractor and to avoid jeoprady of its obligations to the Government, the report may not be released for non-governmental use such as might constitute general publication without the express prior consent of The Ohio State University Research Foundation.

Qualified requesters may obtain copies of this report from the DEFENSE DOCUMENTATION CENTER, Cameron Station, Alexandria, Virginia. Department of Defense contractors must be established for DDC services, or have their "need-to-know certified by the cognizant military agency of their project or contract.

"Distribution of this report is restricted in accordance with the US Export Act of 1949 as amended (DOD Directive 2030.4; AFR 400-10) and it should not be disseminated to OTS".

SOME ASPECTS OF THE TANGENT-ANGLE VS. ARC LENGTH REPRESENTATION OF CONTOURS

Juris G. Raudseps
Communication and Control Systems Laboratory

The Ohio State University
Research Foundation
Columbus, Ohio

TECHNICAL REPORT 1801-6

March 1965

Contract AF 33(615)-1267

Project No. 414408

Task No. 4144

Air Force Avionics Laboratory
Research and Technology Division
Air Force Systems Command
United States Air Force
Wright-Patterson Air Force Base, Ohio

ABSTRACT

A technique is described for characterizing arbitrary, simply connected plane figures by a set of numbers derived from the shape of their outlines. The basis of the description is taken to be the slope of the contour as a function of distance along the contour. This function is expanded in Fourier series, and the series coefficients are taken as a set of descriptors. Topics discussed are the effects of distortion and approximation of contours, reconstruction of figures from their descriptors, and application of the descriptors to pattern recognition. Alternates to the Fourier series expansion of the slope function are also considered.

SOME ASPECTS OF THE TANGENT-ANGLE VS. ARC-LENGTH REPRESENTATION OF CONTOURS

I. Introduction

The significant information in a black-and-white halftone picture field can be represented economically by a set of contours drawn to separate areas of the picture that are everywhere darker than given shades of gray from areas that are everywhere lighter.[1,2,3] For purposes of automatic analysis of pictures, it is desirable to reduce these contours to uniform sets of descriptors, which may then be subjected to various general classification techniques. This report describes the tangent-angle vs. arc-length representation as a basis for generating descriptors for contours, discusses certain aspects of the completeness of the resulting description and its sensitivity to noise, and presents results indicative of its usefulness for classifying shapes.

The tangent-angle vs. arc-length representation of contours has been described in previous reports;[4,5] therefore, only a summary will be given here. Assume an arbitrary closed contour (such as the outline of the letter P in Fig. 1a). Starting at an arbitrary point and going clockwise, plot the angle between the directed tangent to the contour and a reference line as a function of the distance from the starting point measured along the contour. The resulting function (Fig. 1b) is a complete description of the contour in the form of a single-valued function of one variable. It should be noted that logic circuits could readily be built to construct such a description from the information stored in the magnetic core matrix of the ATRID I model.[6]

In its raw form the function described changes shape with a change in the starting point (Fig. 1c). This undersirable dependence can be eliminated quite simply by subtracting from the given function a linear function which decreases by 2π radius in the course of encircling the contour once. The resulting function is now periodic, with a period equal to the length of one circumference. A change in the starting point results in no change in form but only in a shift of the axis. All information about the size of the contour is given by the length of the period, all information about its shape by the form of the function, and all information about its orientation by the combination of the phase and the mean value. With these data is is possible to reconstruct the original contour exactly. If only the shape of the contour is of interest, it is convenient to normalize the length of the period to 2π radian.

A concise numerical description of the form of a contour may be given by the Fourier series coefficients of the tangent angle as a function of the normalized arc length. Several different sets of quantities may be used as the components of an n-dimensional descriptor vector. A set which is independent of the starting point used in tracing the contour consists of merely the magnitudes of the first n harmonic components. While descriptor

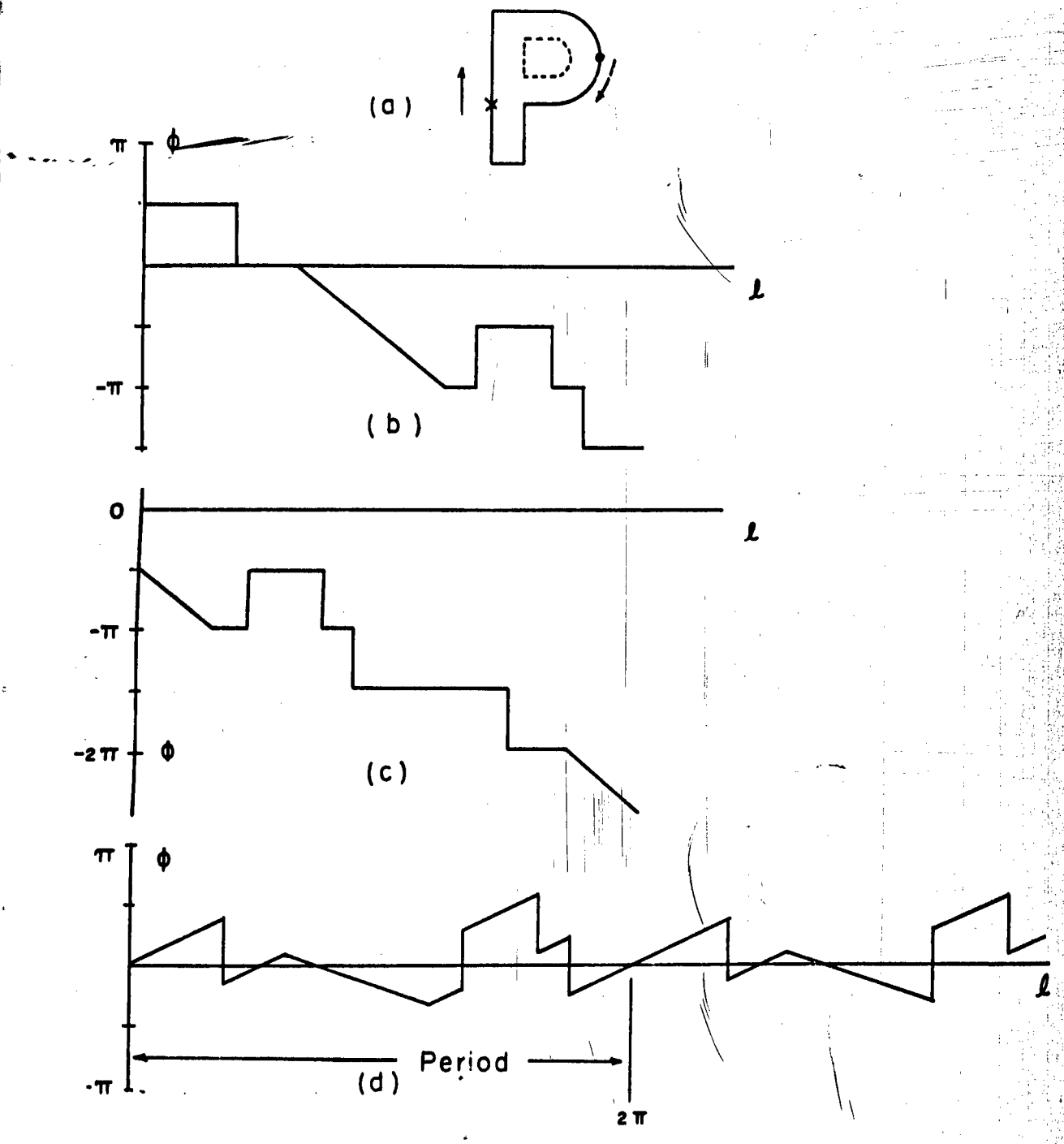

Fig. 1 - A contour (a) and associated $\phi(\ell)$ curves. Curve (b) result of starting to trace contour at cross; curve (c) result of starting at dot. Curve (d) is periodic function obtained by adding ramp function to measured angle $\phi'(\ell)$.

vectors of this type in general do allow meaningful discrimination between contours, they are not the most desirable available, because in the absence of phase information they do not allow even approximate reconstruction of the original contours. Phase information may be retained in either of two ways. In one, the Fourier series representing the contour is expressed in polar form. Then the first n harmonics of the series lead to a descriptor vector of 2n components, of which one-half are measures of amplitude and the other half are measures of phase. In the other, the Fourier series is expressed in cosine-sine form, with alternate components of the descriptor vector representing magnitudes of cosine and sine terms. This latter form is the one that was used in the work to be described. Descriptor vectors of this form contain the information necessary to reconstruct the contours to an accuracy limited only by the number of harmonics considered (see Section III).

II. Approximation of Contours and Noise Considerations

It is important to note that conceptually a tangent-angle vs. arc-length formulation can be found to represent exactly any reasonable contour. In practical applications, it is equally important that adequate approximations to the exact function can be obtained easily and quickly. This section discusses techniques for constructing approximate $\phi(\ell)$ curves and for computing their Fourier series by use of a digital computer. The same concepts used in programming the digital computer to construct the contours could be applied in designing logic circuits to extract contour descriptions from the information stored in the core matrix of the ATRID model.

In principle the approximation used consists of substituting a contour made up of straight-line segments for the exact contour. This has the effect of making the tangent angle ϕ a piecewise constant function of the arc length ℓ (before the ramp function is subtracted).

Because the approximate boundary consists of straight-line segments, the Fourier expansion of its $\phi(\ell)$ function can be calculated very simply. The tangent angle is a piecewise constant function of the circumference. This may be expressed by

$$(1) \qquad \phi'(\ell) = \phi_i \quad \text{for} \quad \ell_{i-1} < \ell \leq \ell_i ,$$

with ϕ_i denoting the angle of the ith line segment. Here $\ell_o = 0$ and ℓ_i is the cumulative length of the first i straight-line segments. Then if the contour is approximated by m segments, ℓ_m equals the total length of the contour L.

The periodic function $\phi(\ell)$ then is

$$(2) \qquad \phi(\ell) = \phi'(\ell) + 2\Pi \frac{\ell}{L} .$$

Proceeding with the Fourier series expansion of $\phi(\ell)$, one may write

$$A_n = \frac{2}{L}\int_o^L \phi(\ell) \cos\left(2\pi n \frac{\ell}{L}\right)d\ell \,, \tag{3}$$

or, in light of Eq. (2),

$$A_n = \frac{2}{L}\int_o^L \phi'(\ell) \cos\left(2\pi n \frac{\ell}{L}\right)d\ell + \frac{2}{L}\int_o^L 2\pi \frac{\ell}{L} \cos\left(2\pi n \frac{\ell}{L}\right)d\ell \,. \tag{4}$$

In order to evaluate the first term of Eq. (4), one may consider the integral over the interval [0,L] as the sum of the integrals over the m sub-intervals $[\ell_{i-1},\ell_i]$. One may then rewrite Eq. (4) as

$$A_n = \frac{2}{L}\sum_{i=1}^{m}\int_{\ell_{i-1}}^{\ell_i} \phi_i \cos\left(2\pi n \frac{\ell}{L}\right)d\ell + \frac{2}{L}\int_{\ell_m}^{L} 2\pi \frac{\ell}{L} \cos\left(2\pi n \frac{\ell}{L}\right)d\ell \,. \tag{5}$$

Evaluating the integrals, one obtains

$$A_n = \frac{1}{n\pi}\sum_{i=1}^{m} \phi_i\left[\sin\frac{2\pi n}{L}\ell_i - \sin\frac{2\pi n}{L}\ell_{i-1}\right] . \tag{6}$$

Since $\sin\left(\frac{2\pi n}{L}\ell_o\right) = \sin\left(\frac{2\pi n}{L}\ell_m\right) = 0$, one may regroup the terms of the summation of Eq. (6) as follows:

$$A_n = \frac{1}{n\pi}\left[\sum_{i=1}^{m-1}\phi_i \sin\frac{2\pi n}{L}\ell_i - \sum_{i=1}^{m-1}\phi_{i+1}\sin\frac{2\pi n}{L}\ell_i\right] \tag{7}$$

to obtain

$$A_n = \frac{1}{n\pi}\sum_{i=1}^{m-1}(\phi_i - \phi_{i+1})\sin\frac{2\pi n}{L}\ell_i \,. \tag{8}$$

Similarly,

$$(9) \qquad B_n = \frac{2}{L}\int_0^L \phi(\ell)\, \sin\left(2\pi\, n\, \frac{\ell}{L}\right) d\ell$$

$$= \frac{2}{L}\sum_{i=1}^{m} \int_{\ell_{i-1}}^{\ell_i} \phi_i\, \sin\left(2\pi\, n\, \frac{\ell}{L}\right) d\ell + \frac{2}{L}\int_0^L 2\pi\, \frac{\ell}{L}\, \sin\left(2\pi\, n\, \frac{\ell}{L}\right) d\ell\,,$$

leading to

$$(10) \qquad B_n = \frac{1}{n\pi}\sum_{i=1}^{m} (\phi_{i+1}-\phi_i)\, \cos\left(\frac{2\pi n}{L}\, \ell + \frac{1}{2\pi n}\right),$$

where

$$(11) \qquad \phi_{m+1} = \phi_1 + 2\pi.$$

Thus it is seen that the Fourier coefficients can be obtained by evaluating sines and cosines at the m points around the contour at which it changes slope and by summing these values, multiplied by the net change in slope at each point.

Preparatory to extracting the approximate contour, a square grid is superimposed on the image. It is convenient to think of the contour not as a line but rather as the boundary between two regions of the field, which we may call "black" and "white." All squares which contain more than some specified fraction of "black" area are assumed to be entirely "black." Boundary squares are then defined as those "black" squares having at least one side in common with a "white" square. Two boundary squares are considered adjacent if they have either a common edge or a common corner. The boundary then is approximated by the straight-line segments connecting the midpoints of successive adjacent boundary squares.

Successive steps in the process of approximating a contour are illustrated in Fig. 2. It should be noted that certain squares may not be boundary squares according to the definition given, even though the actual boundary (but not, of course, the approximate one) passes through them.

Some indication of how the coarseness of the grid affects the quality of the approximation is given by Fig. 3, showing two approximations to the same contour obtained by using grid squares of the size used in Fig. 2 for one and grid squares of half that size for the other. A more definitive criterion for choosing the grid size to be used may be derived from consideration of Fig. 4, which illustrates that if the grid is too coarse, it may depend upon the exact location of a figure relative to the grid whether significant features of the contour appear in the approximation or not.

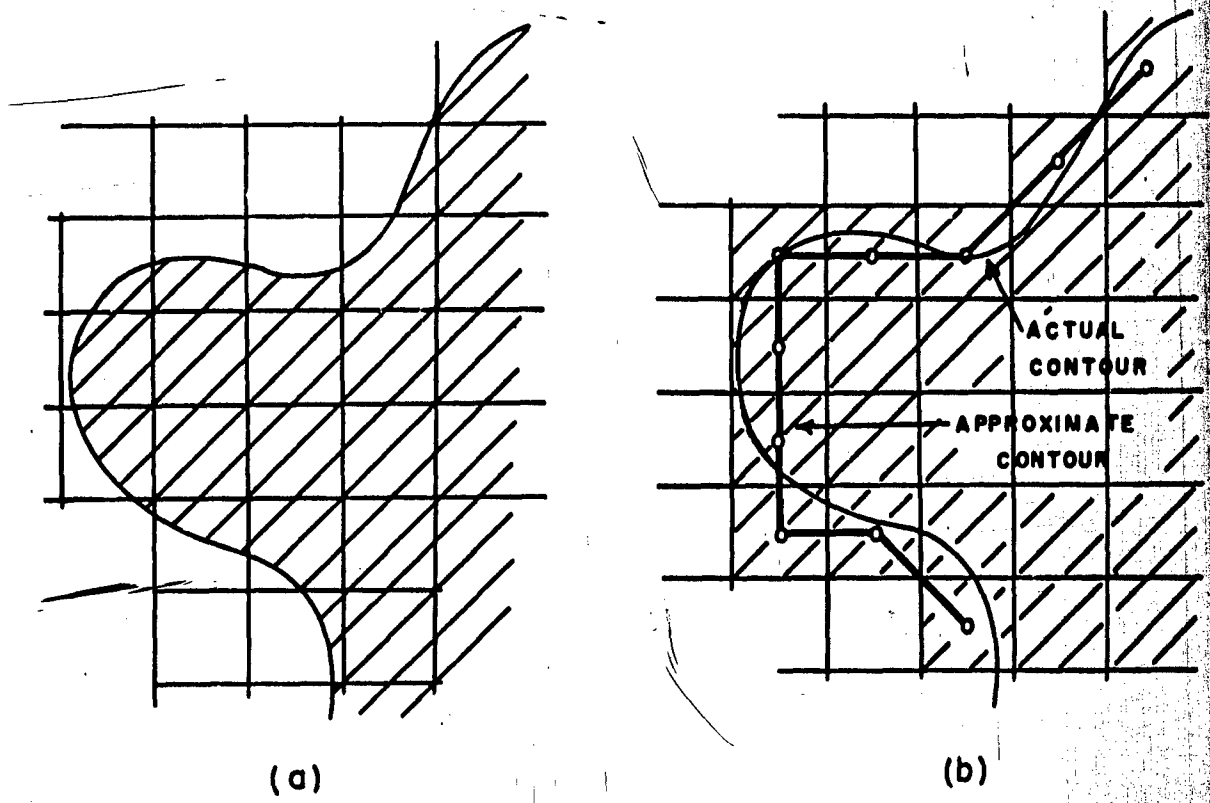

Fig. 2 - Successive steps in approximating a smooth contour by straight-line segments: (a) A grid is laid over the figure. (b) All grid squares partially black originally are made completely black; approximate boundary is constructed by connecting midpoints of black boundary squares.

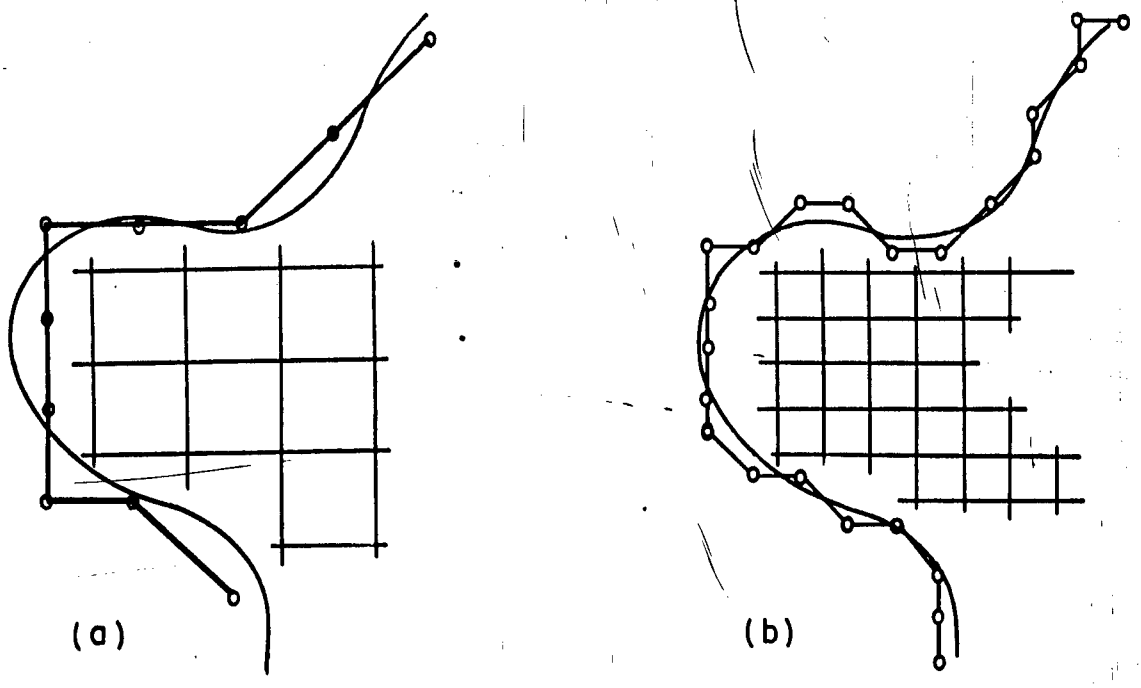

Fig. 3 - Approximate boundary drawn with coarse grid (a) and with fine grid (b).

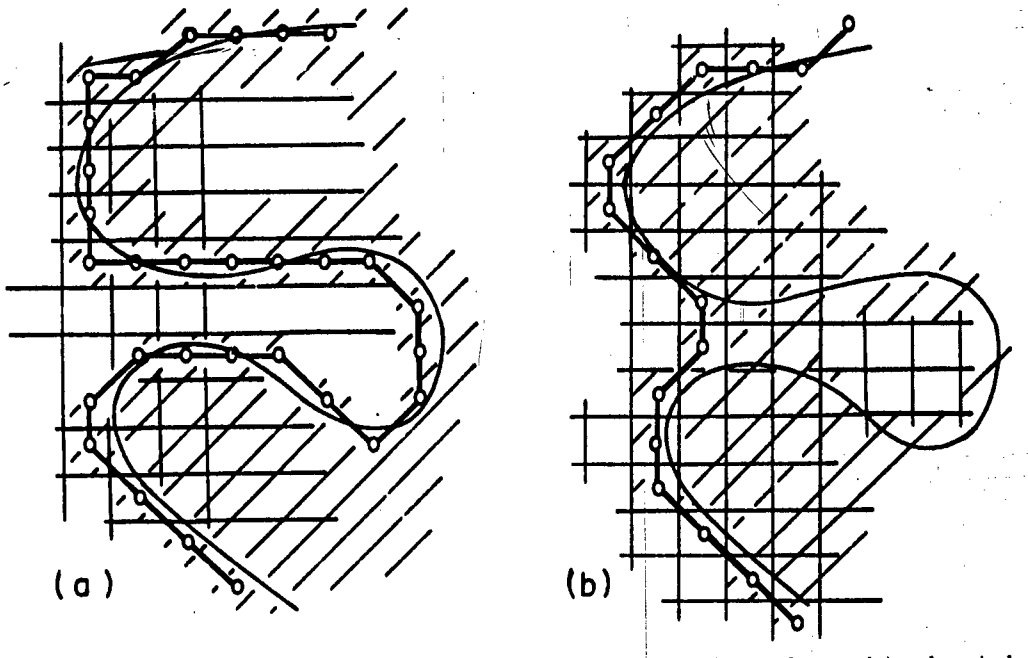

Fig. 4. Variations in detail of approximate contour brought about by shifting grid. Indentation in original contour is reproduced in approximation with grid placed as in (a), missed with grid placed as in (b).

It is clearly desirable that fixing the grid size should determine the mimimum size of detail to appear in the approximate contour. Variations in the detail because of random placing of the original contour relative to the grid, as between Fig. 4a and Fig. 4b, must be considered a type of noise. Such noise has two effects upon the $\phi(\ell)$ function. First, the magnitude of the tangent angle ϕ is changed in the vicinity of the distortion of the contour. Second, the length of the contour is changed. The second effect is the more important, for if distortions of one part of a contour significantly change its length while the rest of the contour is unchanged, the overall form of the $\phi(\ell)$ function may be greatly altered (Figs. 5 and 6), with an attendant effect upon the Fourier series coefficients.

The fact that noise of the type described does change both the "dependent" and the "independent" variable in the $\phi(\ell)$ representation (which, incidentally, means that the noise is not additive) changes the very nature of the filtering problem. Superimposed noise caused by irrelevant fine detail might be removed by a low-pass filter. In fact, since only a limited number of harmonics are considered in the Fourier series expansion, the process of extracting descriptors would by itself remove the high-frequency noise components. Under the actual circumstances, no linear filtering of the $\phi(\ell)$ function is useful for reducing the noise caused by distortions. Instead, the smoothing process must be carried out on the actual contour.

Smoothing and approximation of a given contour are, in principle, different operations. In practice, they are readily combined. The purpose of smoothing is to replace by smooth arcs those sections of a contour containing irrelevant fine detail. The purpose of approximation is to reduce curved contours to straight-line segments bound to a grid. The combined smoothing-approximating operation ideally should transform a given contour containing detail finer than that desired to a straight-line approximation, with all the detail finer than some specified size eliminated and all coarser features indicated rather faithfully.

It must be realized that the ideal described above cannot be achieved. Any process incorporating a quantizing step is subject to quantizing noise. Here it will manifest itself in the unreliability of the designation of a square on or near the actual contour as "white" or "black." Thus the "size" of a given piece of detail cannot be fixed exactly, and it is not possible to distinguish in all cases between "fine irrelevant detail" to be smoothed out and "significant features" to be retained. The criterion for smoothing must therefore be based, here as in other cases, upon the likelihood that certain classes of features are in error and upon the seriousness of the influence such error might have upon the descriptors.

No quantitative description of noise effects is available. Qualitatively, it may be said that the most probable noise consists of irregular serration of the boundaries between areas and other minor discontinuities in the contours. The effect of such noise may be to obscure the gross features of the contour, as illustrated in Figs. 5 and 6.

The smoothing-approximation technique developed to minimize the effects

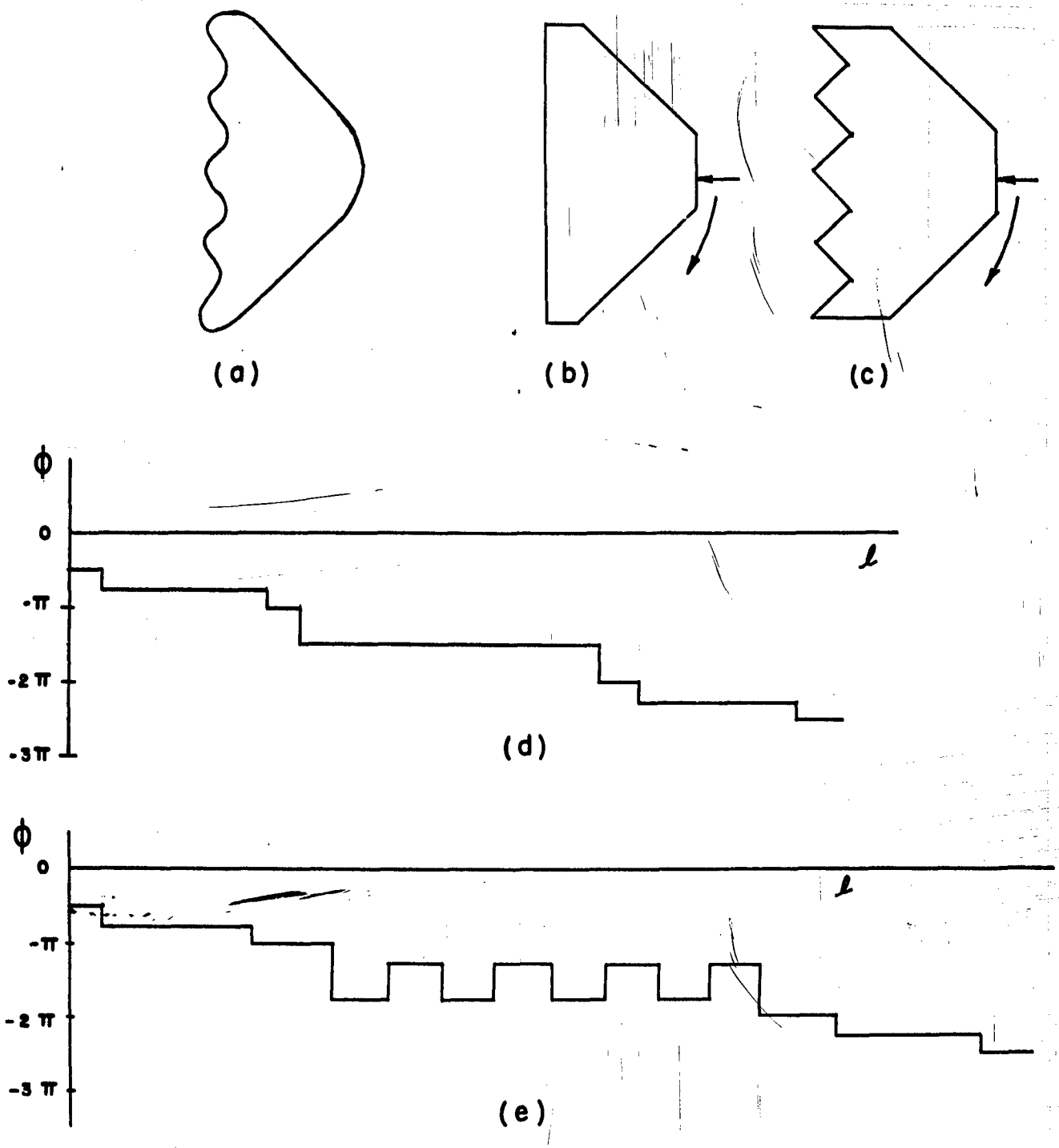

Fig. 5 - Effects of noise introduced by serrations of contours: (a) Contour, (b,c) two possible approximations. Tangent angle as function of distance along contour for approximation (b) is shown by (d) and for approximation (c) by (e).

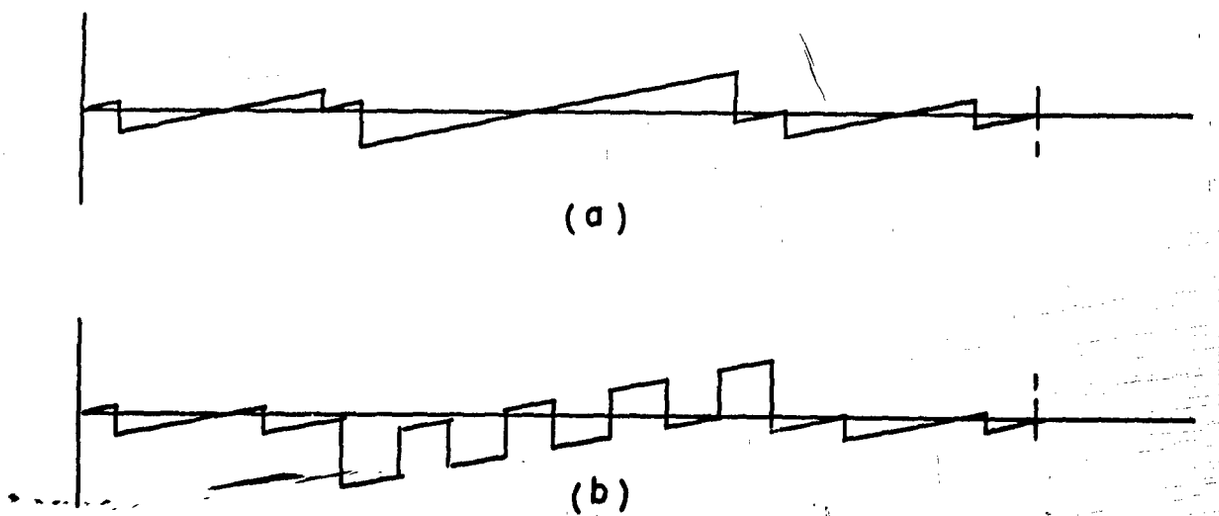

Fig. 6 - Normalized, periodic $\phi(\ell)$ functions obtained from the two approximations (Figs. 5b, 5c) to the contour of Fig. 5a. A difference in the harmonic content is quite evident.

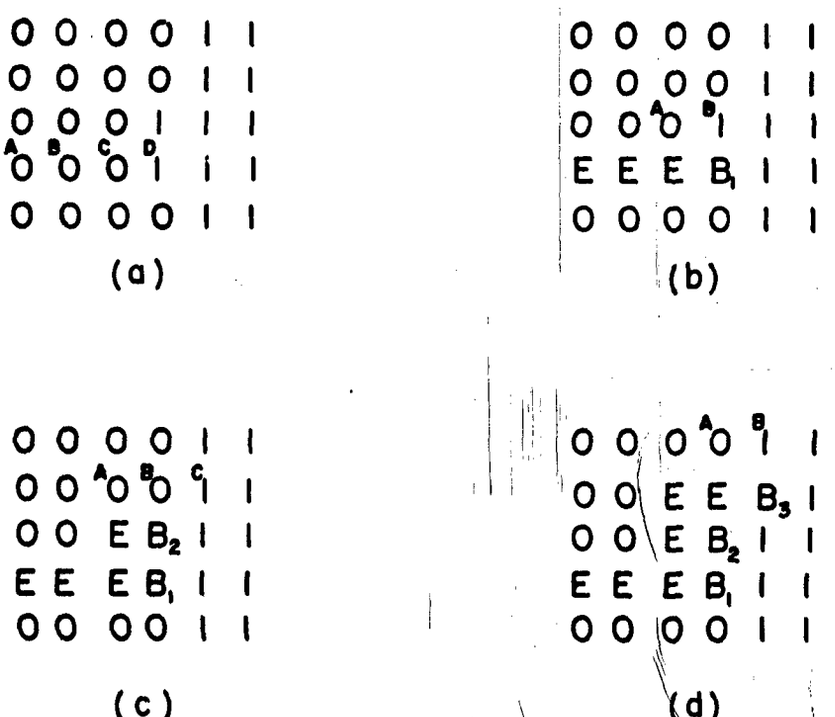

Fig. 7 - Successive steps in tracing approximate outline of a figure stored in computer memory as a zero-one matrix. E's denote elements examined and found zero; B_i's denote successive boundary squares; small superscripts show order in which tests are performed.

of such noise will now be described in terms of its digital-computer implementation. Subsequently, some indication will be given of how the same results could be obtained working with the ATRID device.

A given figure is stored in computer memory as a zero-one matrix, each "zero" element representing a "white" square and each "one" element representing a "black" square. The first boundary square is found by scanning a given line of the matrix until a "one" element is found. If no smoothing is to be performed, the elements corresponding to adjacent squares are examined in clockwise order until another "one" is found. This corresponds to the next boundary square. The squares adjacent to it are again examined in clockwise order, and so forth. Figure 7 shows successive steps of the search.

Smoothing of a contour is achieved by changing certain initially "white" squares to "black" if such change could effect a straightening of a piece of a contour by filling in breaks or gaps. The criterion for the change is established as follows: Assume a particular boundary square is given. Examine in clockwise order the squares beyond the immediately adjacent ones. The first one to be found black will be a boundary square also. It is desired that the boundary between these two points be straight. Accordingly, the intervening squares are made black if necessary, so as to allow them to be boundary squares. The approximation then proceeds as before; the squares adjacent to the last square of the approximate contour are examined in clockwise order, and the boundary is extended to the midpoint of the first one found to be "black."

Figure 8 shows successive steps of the combined smoothing-approximating process. The process illustrated will smooth out detail of size on the order of one or two squares. This appears to correspond to the most reasonable combination of choice of grid size and definition of extraneous detail. It is the only smoothing scheme actually programmed. It is clear, however, that the concept could be extended to examining squares further away and changing to black more than one square on the basis of one examination.

Figure 8a shows the scanning process, which is the same as that in Fig. 7a. Figs. 8b, d, f, and h show the order of searching ahead for a boundary square. In Figs. 8c, e, g, and i the X indicates the square thus found, and the starred "one" is that element which must as a consequence correspond to a "black" square if the contour is to be smooth. It may be noted that in all but Fig. 8g, the starred element was "one" initially. It may also be noted that the starred element in Fig. 8e does not correspond to a boundary square, because the clockwise search about B_2 detects another "one" element first.

If the ATRID device were to be used for tracing contours, a somewhat different procedure would apply. In the ATRID core matrix, the cores containing ones are those corresponding to grid squares in which there occurs the transition from one level to another, i.e., from "black" to "white" or "white" to "black." These are boundary squares. Formally this definition

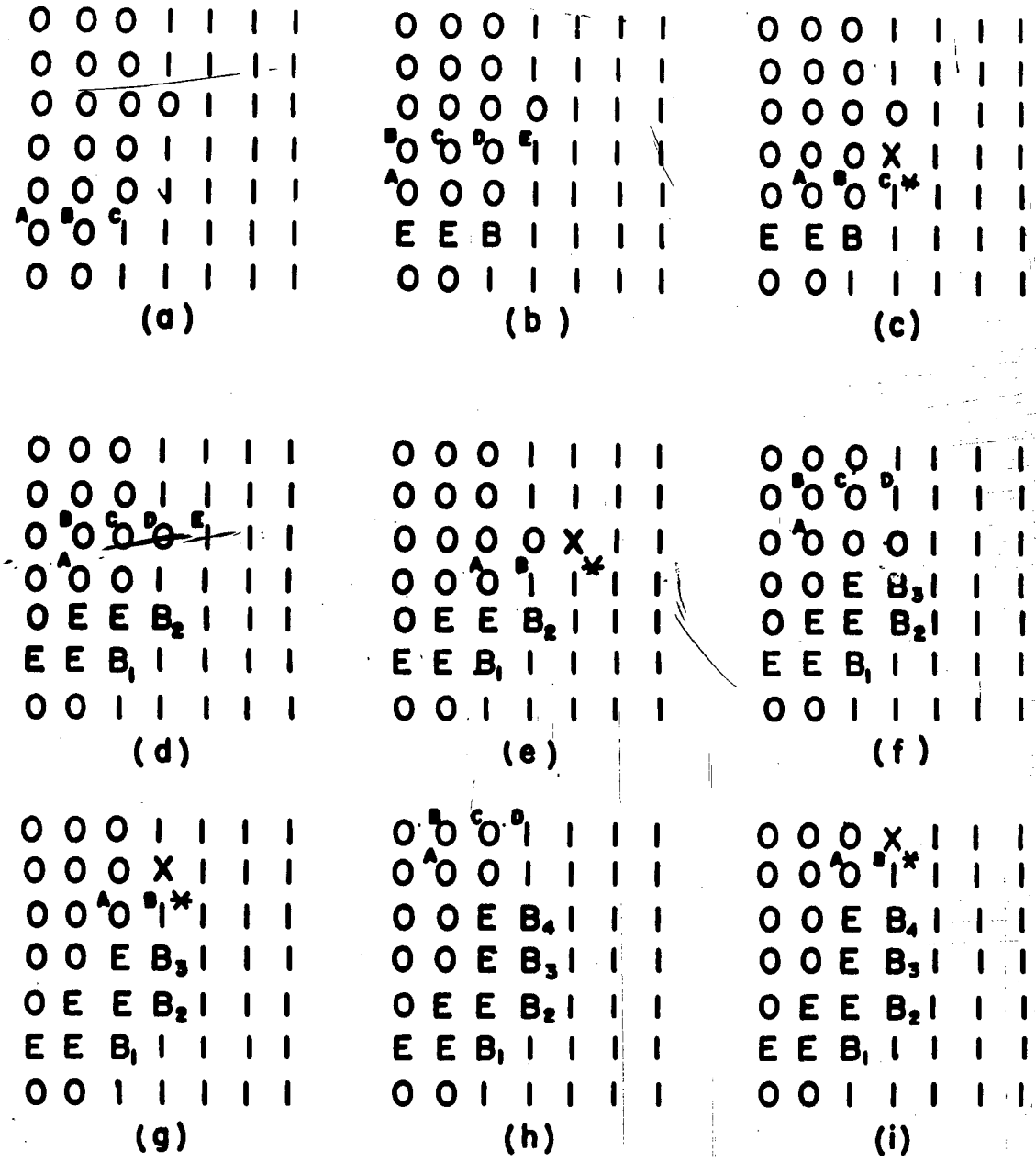

Fig. 8 - Successive steps in process that combines smoothing and approximation of the outline of a figure stored in computer memory as a zero-one matrix.

of "boundary square" is different from that previously given, but in practice there is no real difference. For the operation of curve tracing, a core known to be on the boundary could be interrogated while successively paired with the cores adjacent to it. If smoothing were to be performed also, the cores could be interrogated in sets of three, with pulses large enough to give a response if any two of the cores were set.

III. Reconstruction of Figures from Their Descriptors

The normalized tangent-angle vs. arc-length curve is a complete description of the shape of a figure. Any truncated Fourier series representation of this curve can be only an approximate description. Since the descriptor vector used to characterize and classify a given contour consists of the coefficients of such a truncated Fourier series, it is of interest to know how the number of harmonics present affects this description.

A computer program was written to reconstruct a contour, given the descriptor vector with a specified number of components. Basically, the computer is programmed to construct a contour of the same form as the approximate contours discussed previously; that is, one consisting of straight-line segments connecting the midpoints of adjacent grid squares. The coarseness of the grid may be adjusted by specifying the length to be assumed for the contour in terms of grid squares. The program proceeds by evaluating the Fourier series at the approximate midpoint of the next segment to be considered. (The exact midpoint is unknown, a priori, because the segment length may be either 1 or $\sqrt{2}$ units.) The value of the angle computed at this point is rounded to the nearest of the eight possible values, and the contour is extended by a line increment at that angle. An effort is made to prevent roundoff error from accumulating, in that a correction term equal to the roundoff error at the previous point is added to the angle computed at a given point.

It is clear that this reconstruction technique yields only an approximation to the contour actually specified by the Fourier coefficient descriptors. The approximation becomes exact in the limit as the grid becomes infinitesimally fine. The accuracy of the approximation may be judged by comparing two reconstructions of the same figure based on the same descriptors, with one having a grid twice as fine as the other (Fig. 9).

Figures 10-12 show several contours reconstructed on the basis of various numbers of harmonics.

IV. Standardization of Phase

It has been shown in Sections I that a given contour can be reduced to a $\phi(\ell)$ curve which is periodic and the shape of which is independent of the

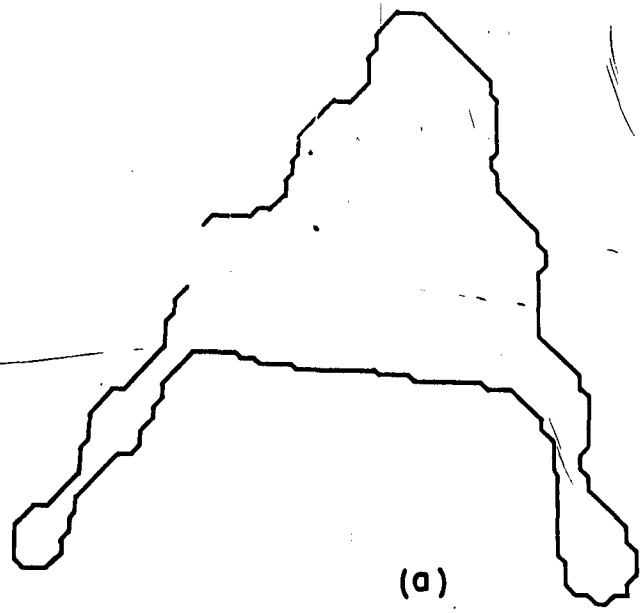

(a)

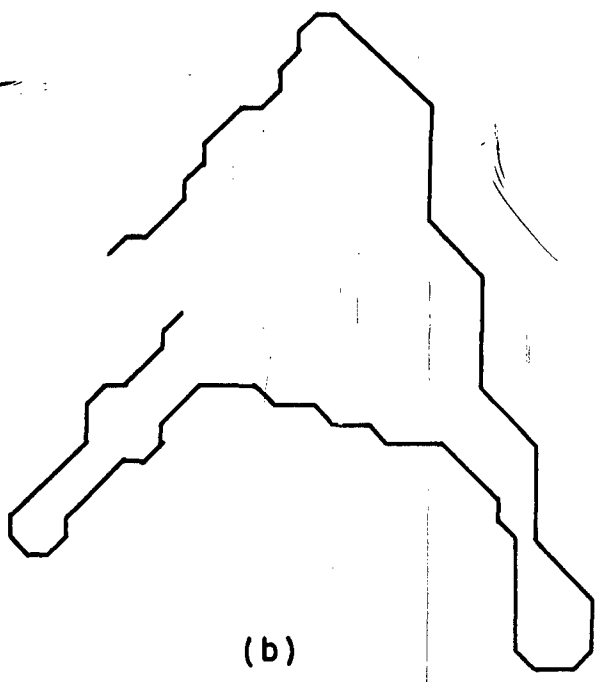

(b)

Fig. 9 - Two reconstructions of the same figure from a descriptor vector of 30 components (cosine and sine coefficients of first 15 harmonics). The reconstruction shown in (a) is based on the calculation of the slope of the contour at roughly twice as many points as the reconstruction in (b).

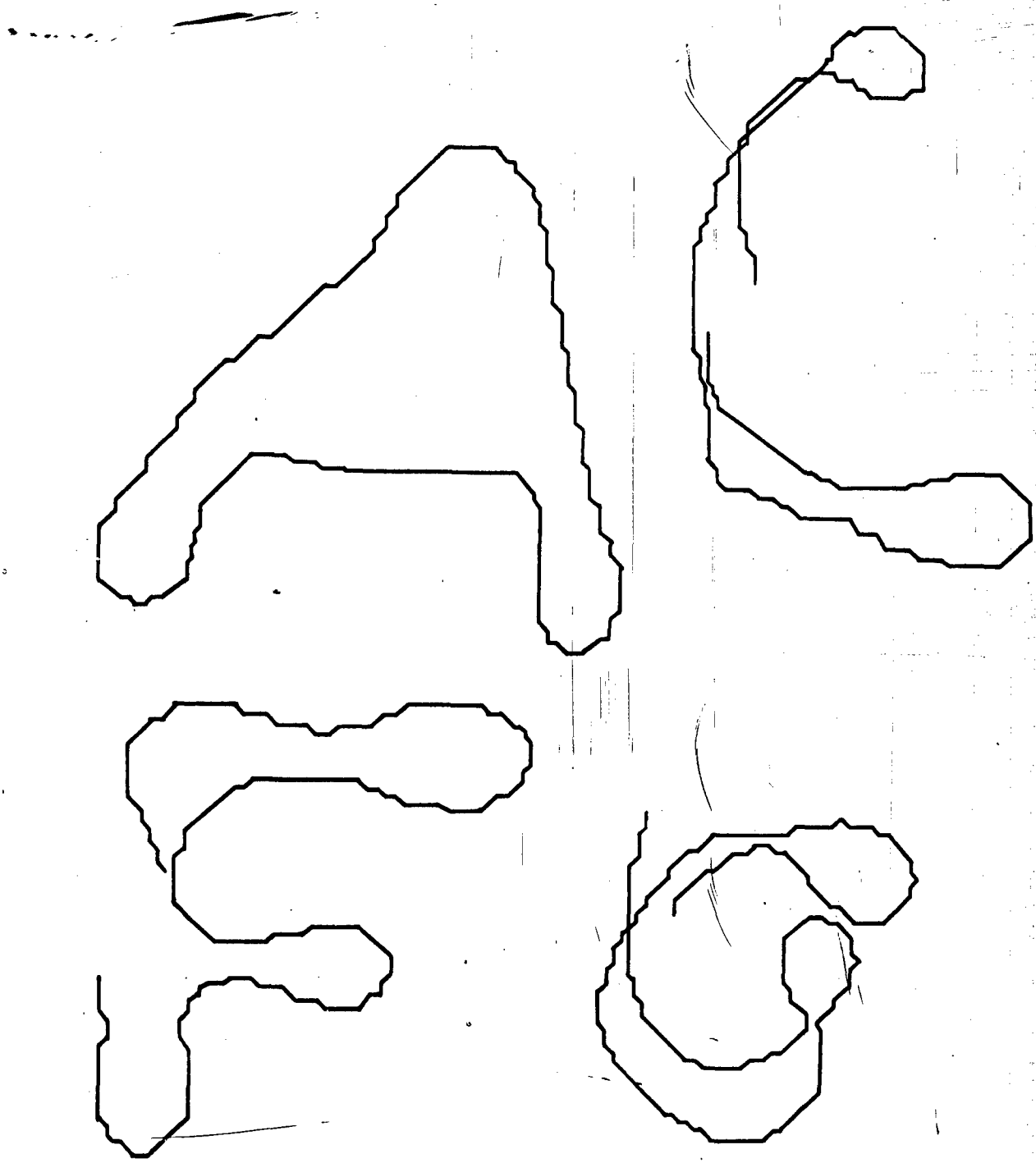

Fig. 10 - Characters reconstructed from descriptor vectors consisting of the cosine and sine coefficients of the first 6 harmonics.

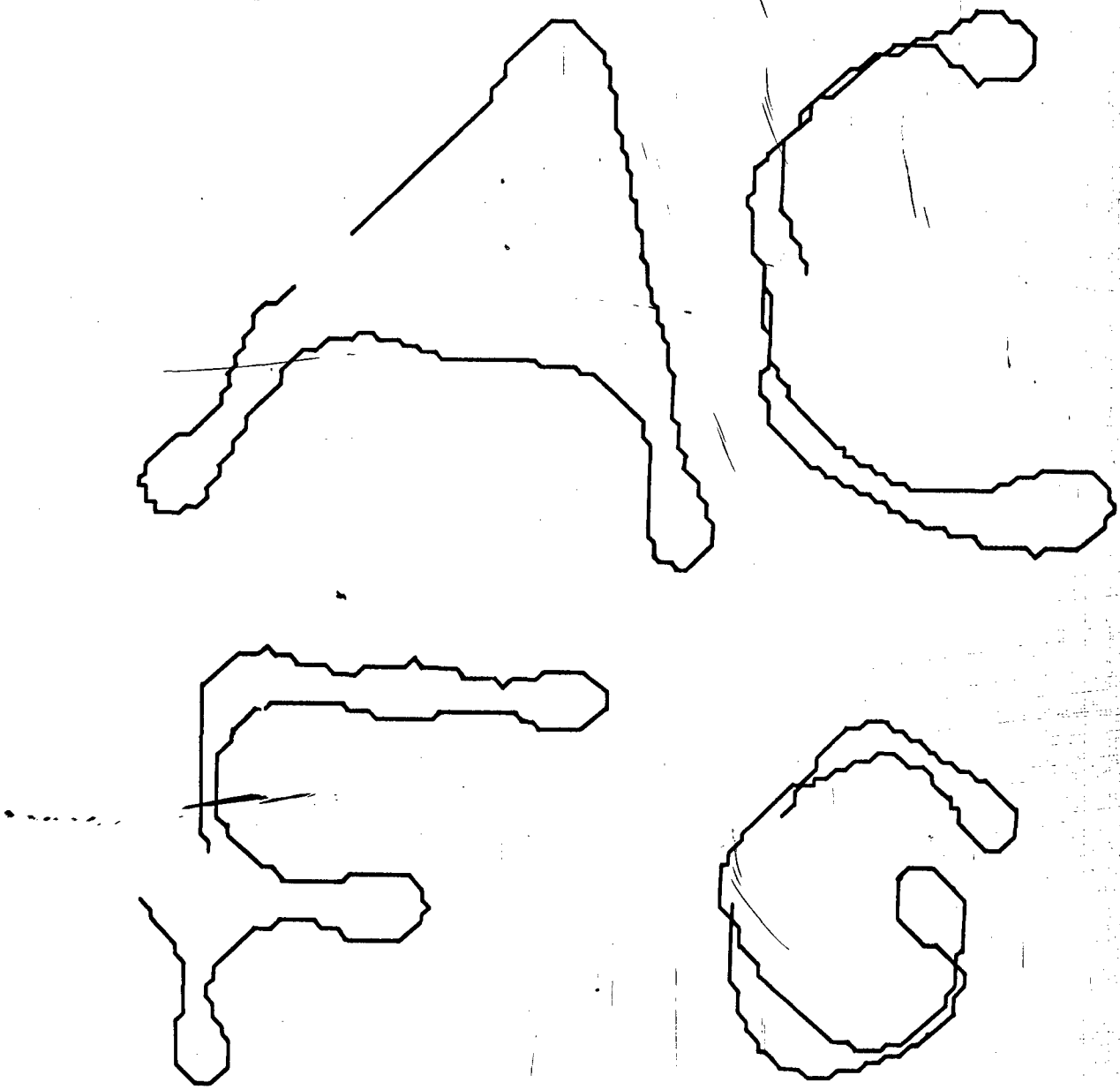

Fig. 11 - Characters reconstructed from descriptor vectors consisting of the cosine and sine coefficients of the first 10 harmonics.

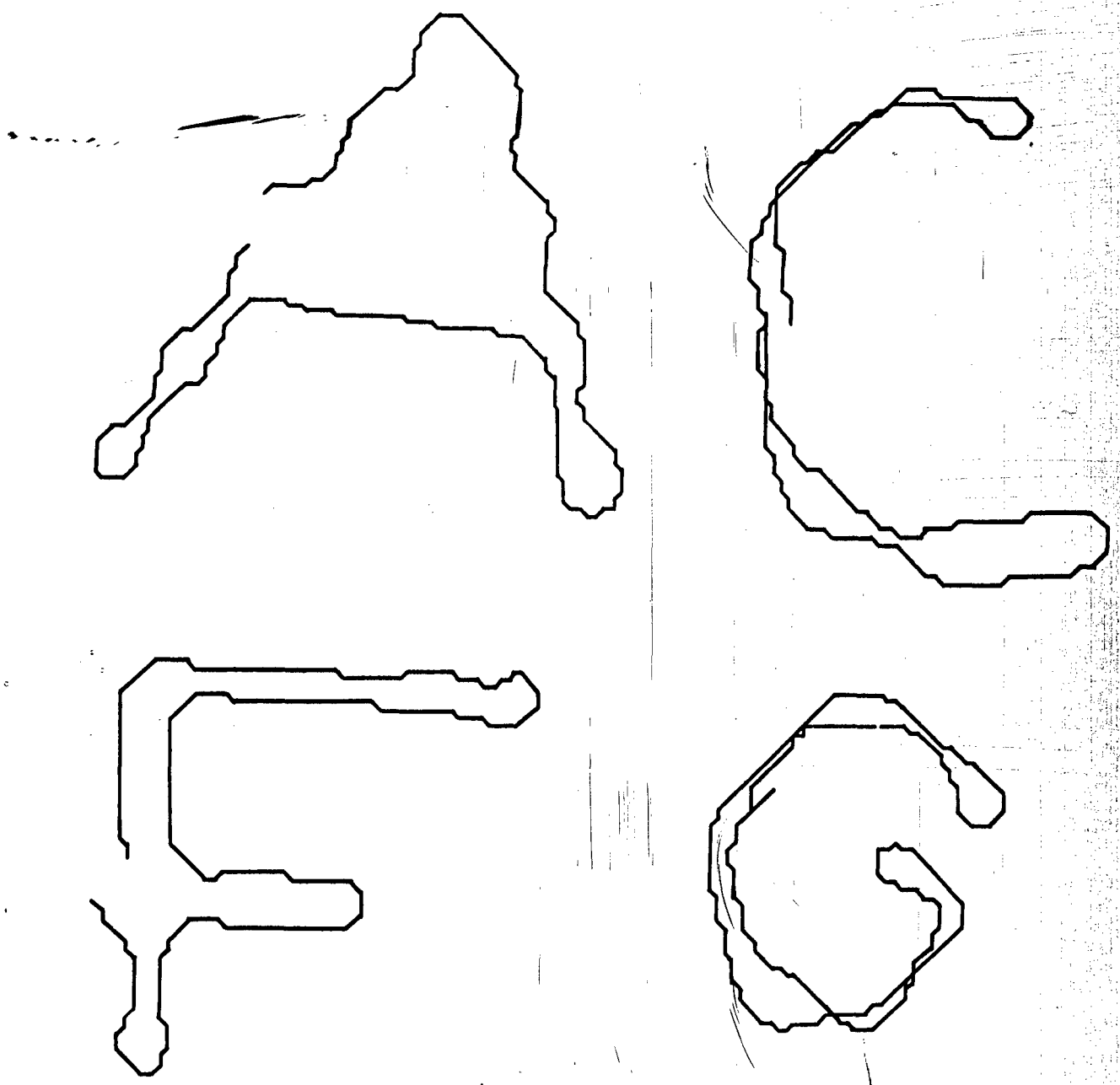

Fig. 12. Characters reconstructed from descriptor vectors consisting of the cosine and sine coefficients of the first 15 harmonics.

starting point used in tracing the contour. The amplitude and the relative phase of each harmonic are thus fixed. However, the absolute phase may vary arbitrarily, depending upon the starting point selected for tracing the contour. A descriptor vector consisting of Fourier series coefficients may be constructed, no matter what starting point is chosen. All such descriptor vectors are "correct" and equivalent in that the figure which can be reconstructed with a given number of harmonics is the same. (It is assumed that enough harmonics are taken for the contour to close; obviously any break in the contour will occur at the starting point selected.)

If the descriptor vectors are to be used to classify figures, some restraint on the starting point must be imposed. Classification techniques depend upon grouping the end-points of n-dimensional vectors in n-space. Objects described by descriptor vectors are recognized as being similar if their vectors fall in the same region of n-space. If the starting point for tracing the contour is allowed to vary arbitrarily along the contour, a single given contour will lead to a set of descriptor vectors specifying points in n-space the locus of which will be a rather complex curve. Its projection on any one axis will range between the positive and negative value of the amplitude of the associated harmonic. It is therefore clear that uncontrolled variation of the starting point used for tracing contours makes meaningful comparison of descriptor vectors quite difficult.

Fortunately, any descriptor vector obtained upon starting to trace a contour at an arbitrary point can be transformed to any of the other possible descriptor vectors by a completely determinate linear transformation. A shift in starting point amounts to merely a shift in phase of the periodic $\phi(\ell)$ curve. Consider a given 2n dimensional descriptor vector, consisting of n pairs of cosine coefficients, A_i, and sine coefficients, B_i:

(12) $$\underline{V} = A_1, B_1, ---, A_i, B_i, ---, A_n, B_n.$$

Then

(13) $$C_i = \sqrt{A_i^2 + B_i^2}$$

and

(14) $$\phi_i = \tan^{-1} \frac{B_i}{A_i} ;$$

and conversely

(15a) $$A_i = C_i \cos \phi_i$$

and

(15b) $$B_i = C_i \sin \phi_i .$$

For any two vectors, $\underline{V}^a$ and $\underline{V}^b$, describing the same contour,

$$C_i{}^a = C_i{}^b, \tag{16}$$

since the harmonics are of the same magnitude. However, in general

$$\phi_i{}^a = \phi_i{}^b + \theta_i, \text{ where } \theta_j \neq 0. \tag{17}$$

Similarily, for another harmonic

$$C_j{}^a = C_j{}^b \tag{18}$$

and

$$\phi_j{}^a = \phi_j{}^b + \theta_j \ , \tag{19}$$

and, because of the geometrical interpretation of the quantities,

$$\theta_j = \frac{j}{i}\theta_i \ . \tag{20}$$

By Eq. (20) the phase shift of every harmonic can be computed if it is known for any one. Thus, an apparent change in the starting point can be achieved by operations upon the descriptor vector.

The standard starting point to be used in developing vectors for the classification of contours must be specified in terms of properties of the vectors, since no salient features of the contours themselves are known a priori. For obvious reasons this starting point must be unique. It must be specified in terms of the phase angles of the harmonics. As a practical matter, the contour may be traced starting at any convenient point, and a virtual shift of the starting point may be brought about by means of transformations derived from the equations given above.

A starting point may be uniquely specified by the requirement that either the phase angle of the fundamental or some function of the phase angles of several harmonics assume a specified value, which may be zero. Specification of a starting point in terms of the phase angle of any one harmonic, other than the fundamental, does not lead to a unique result, since any given phase angle occurs at several points around the contour.

Specification in terms of the fundamental harmonic alone is unsatisfactory because the amplitude of that harmonic may be zero for certain figures (e.g., any regular polygon) and the angle may be indeterminate. Two different

criteria for specifying the starting point in terms of the phase angles of all the harmonics to be considered were tried. The restrictions imposed were that the starting point be selected such that either

$$\sum_{i=1}^{n} C_i \phi_i = 0 \tag{21}$$

or

$$\sum_{i=1}^{n} \frac{C_i}{i} \phi_i = 0. \tag{22}$$

In each case each phase angle was weighted by the corresponding amplitude in order to eliminate the difficulties that would arise if a given harmonic were identically zero, with indeterminate phase, or of such small amplitude that very minor perturbations of the contour could change the phase over a wide range.

The criterion for accepting a given way of specifying the starting point as good is that descriptor vectors of similar figure be consistently closely grouped. To test the two bases for selecting starting points given by Eqs. (21) and (22), several sets of contours were generated and their descriptor vectors compared.

Three different objects (models of an A3J aircraft, a B47 bomber, and a T34 tank) were photographed from a wide range of azimuth and elevation angles. Their silhouettes were traced and the first six harmonics of the Fourier series expansion of their tangent-angle vs. arc-length description were computed. Transformations were performed upon the resulting descriptor vectors to obtain both a set of vectors satisfying the requirements of Eq. (21) and another set satisfying Eq. (22).

To obtain some indication of how the end-points of these vectors clustered in the descriptor space, projections of that 12-space upon a set of mutually perpendicular planes were plotted. In particular, out of the 66 possible planes, those six were chosen which resulted in the sine coefficient of each harmonic being plotted against the cosine coefficient. It was found that the vectors satisfying

$$\sum_{i=1}^{n} \frac{C_i}{i} \phi_i = 0 \tag{22}$$

appeared very closely grouped in the projections upon the A_k-B_k planes for

small k, but were quite widely scattered for larger k (Figs. 13 and 14). For this reason the criterion of Eq. (22) may be considered inferior to that of Eq. (21).

The clustering resulting from imposition of the requirement

$$\sum_{i=1}^{n} C_i \phi_i = 0 \tag{21}$$

is shown in Figs. 15-20.

It should be noted that the clusters for the A3J and the B47 are both disjointed from that for the T34 in the A_1 - B_1 plane, and the clusters for the A3J and the B47 are disjointed in the A_3 - B_3 plane. Thus an unknown object from one of these clusters could be tentatively identified from the projection of its descriptor vector upon these two planes. It should also be noted that this disjointedness is not evident from the graph showing the range of individual components of the descriptor vectors for the various targets (Fig. 21).

V. Pattern Recognition

The term descriptor will be used to denote a number whose value is a measure of the degree to which the figure under consideration possesses a certain property. This number may be a binary one or zero, denoting the presence or absence of some specific feature and thus giving an essentially qualitative description of the figure; or the number may assume a value proportional to some characteristic of the figure which may be specified quantitatively. No restriction is placed on the properties that may be characterized by descriptors. They may be features that can be recognized by inspection (e.g., whether the figure falls into a certain region of a superimposed grid), by simple measurement (e.g., height, width), or by arbitrarily complex computation based on any number of physical measurements (e.g., height-to-width ratio). Because of the variety of different quantities that the term must designate, the work "descriptor" appears more suitable then "measurement," which has also been used in this sense.[7] When a set of several descriptors pertaining to a given figure is to be used, it is convenient arrange them in a fixed order. Such an ordered set of descriptors will b called a descriptor vector.

Regardless of how the descriptor vectors are obtained, they are useful for character or pattern recognition if, and only if, the following two requirements are satisfied: (1) It is easier to perform comparisons of the descriptor vectors than of the figures themselves, and (2) the descriptor vectors of similar figures appear similar under the comparisons performed.

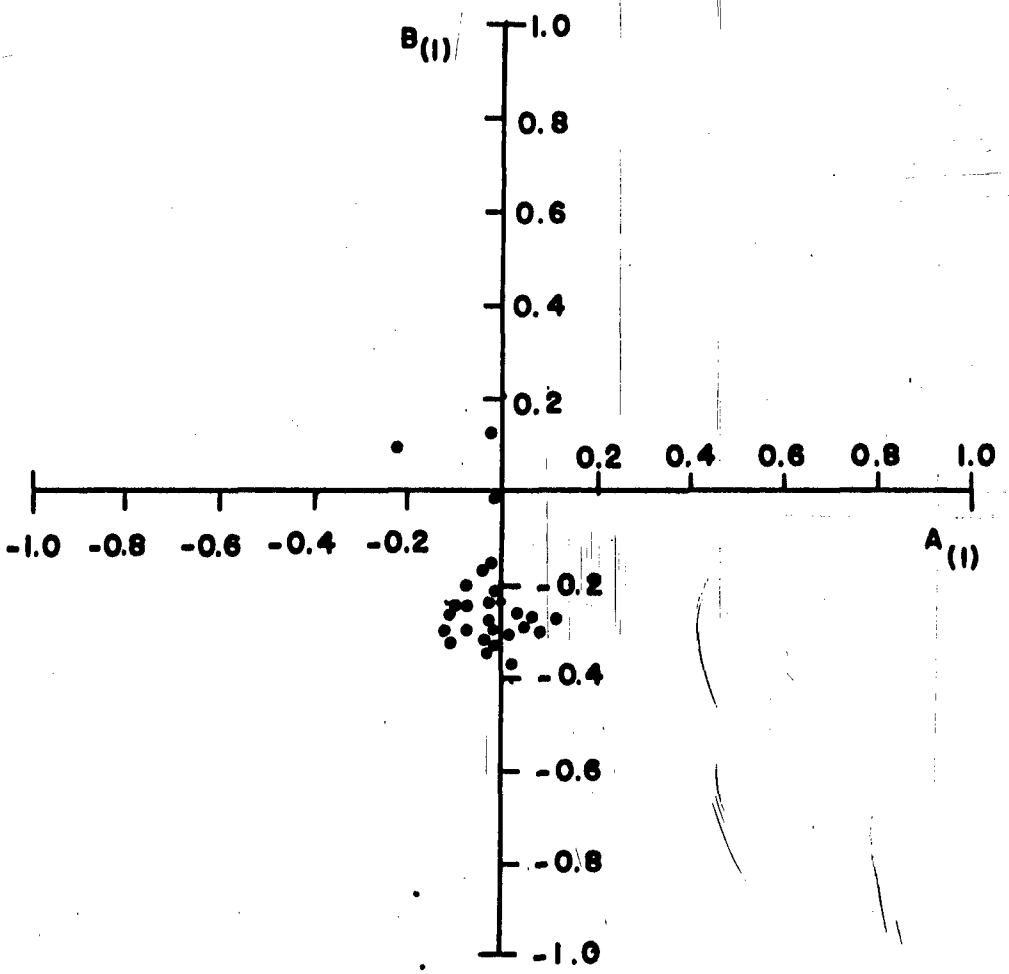

Fig. 13 - Projection of descriptor vectors of T34 tank upon the plane of the cosine and sine coefficients of the first harmonic. Descriptor vectors have been adjusted to satisfy Equation 22.

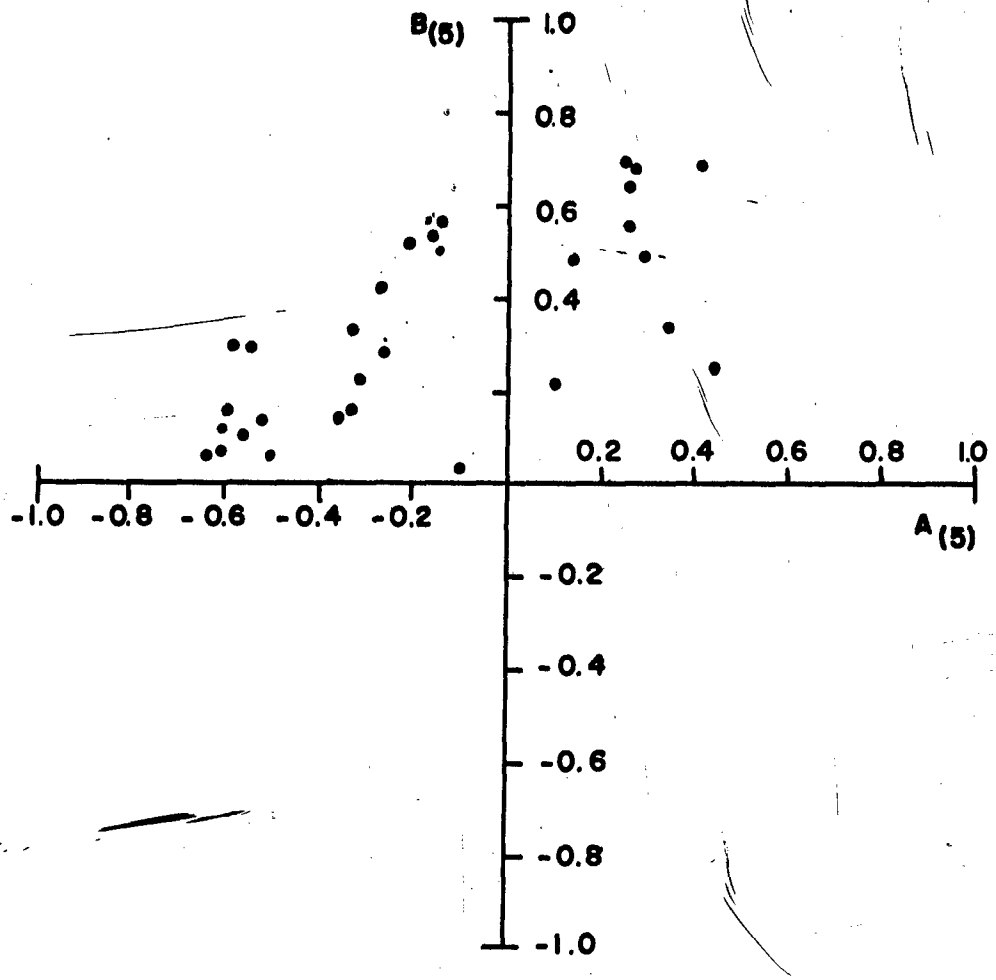

Fig. 14 - Projection of descriptor vectors of T34 tank upon the plane of the cosine and sine coefficients of the fifth harmonic. Descriptor vectors have been adjusted to satisfy Equation (22).

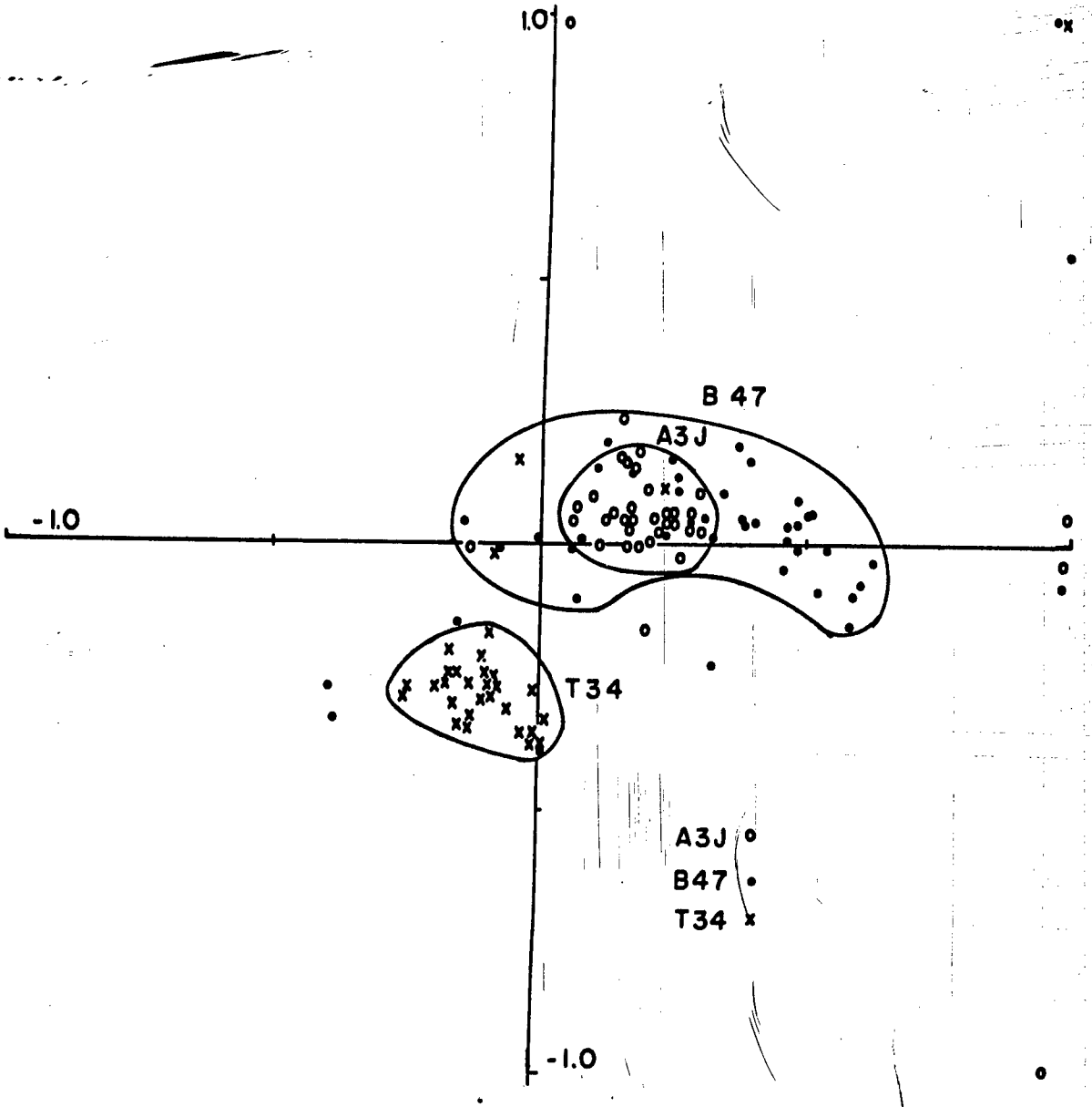

Fig. 15 - Projection of descriptor vectors of three objects viewed from various orientations upon the plane of the cosine and sine coefficients of the first harmonic. Descriptor vectors have been adjusted to satisfy Eq. (21). Note that cluster of T34 tank is disjointed from clusters of both aircraft.

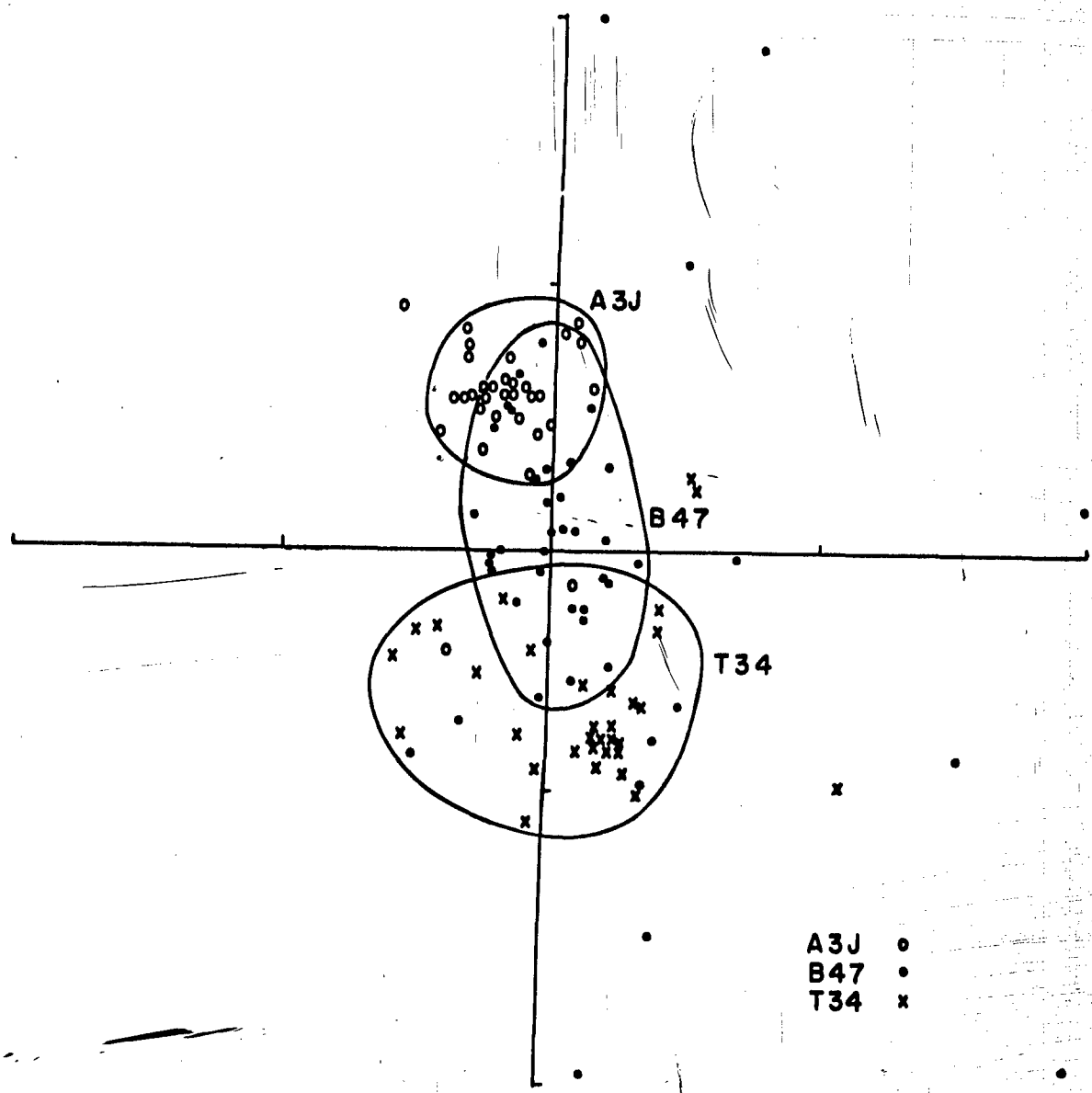

Fig. 16 - Projection of descriptor vectors of three objects upon the plane of cosine and sine coefficients of the second harmonic. Descriptor vectors satisfy Eq. (21).

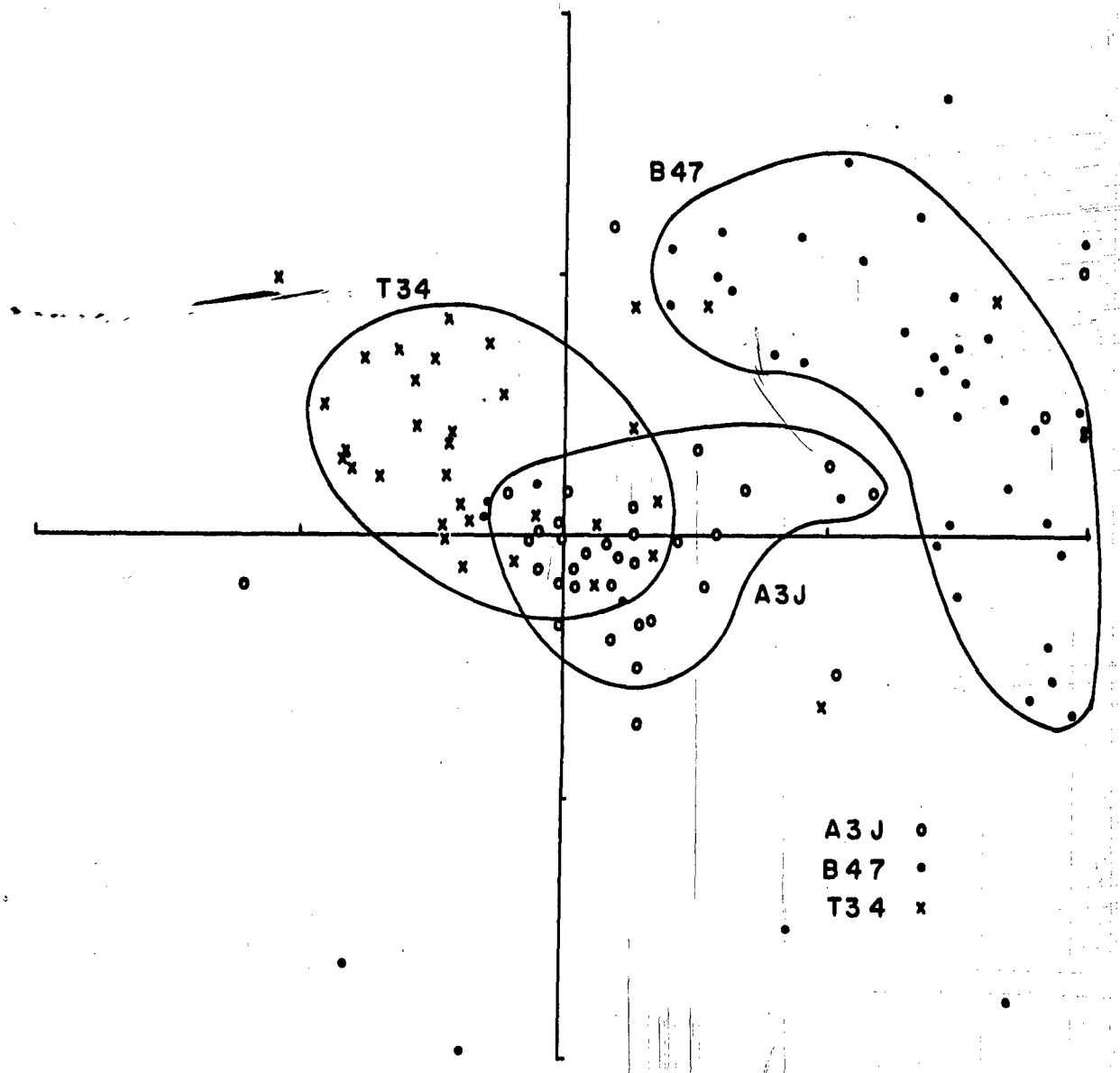

Fig. 17 - Projection of descriptor vectors of three objects upon the plane of cosine and sine coefficients of the third harmonic. Descriptor vectors satisfy Eq. (21). Note that clusters for the two aircraft are disjointed.

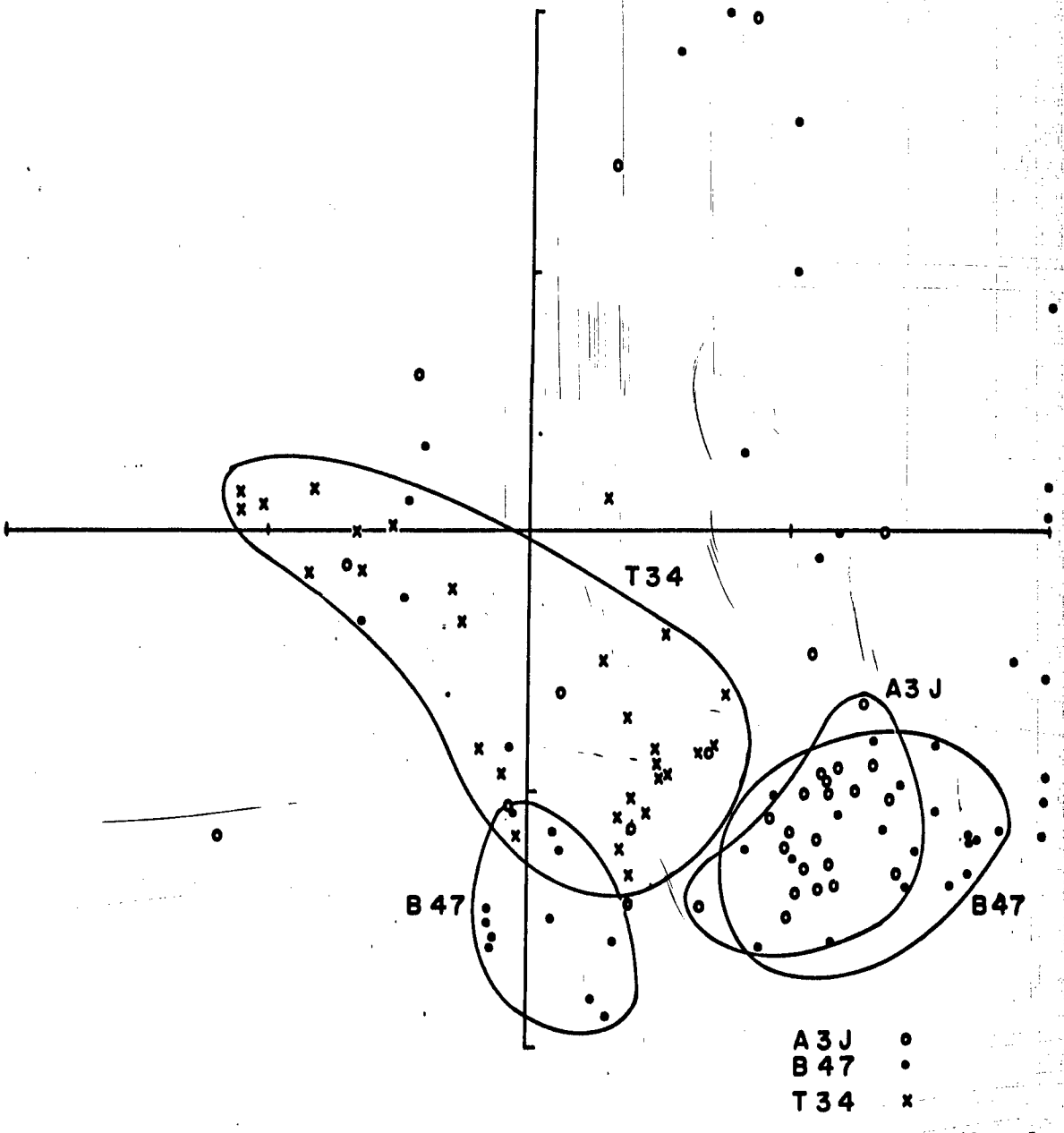

Fig. 18 - Projection of descriptor vectors of three objects upon the plane of cosine and sine coefficients of the fourth harmonic. Descriptor vectors satisfy Eq. (21).

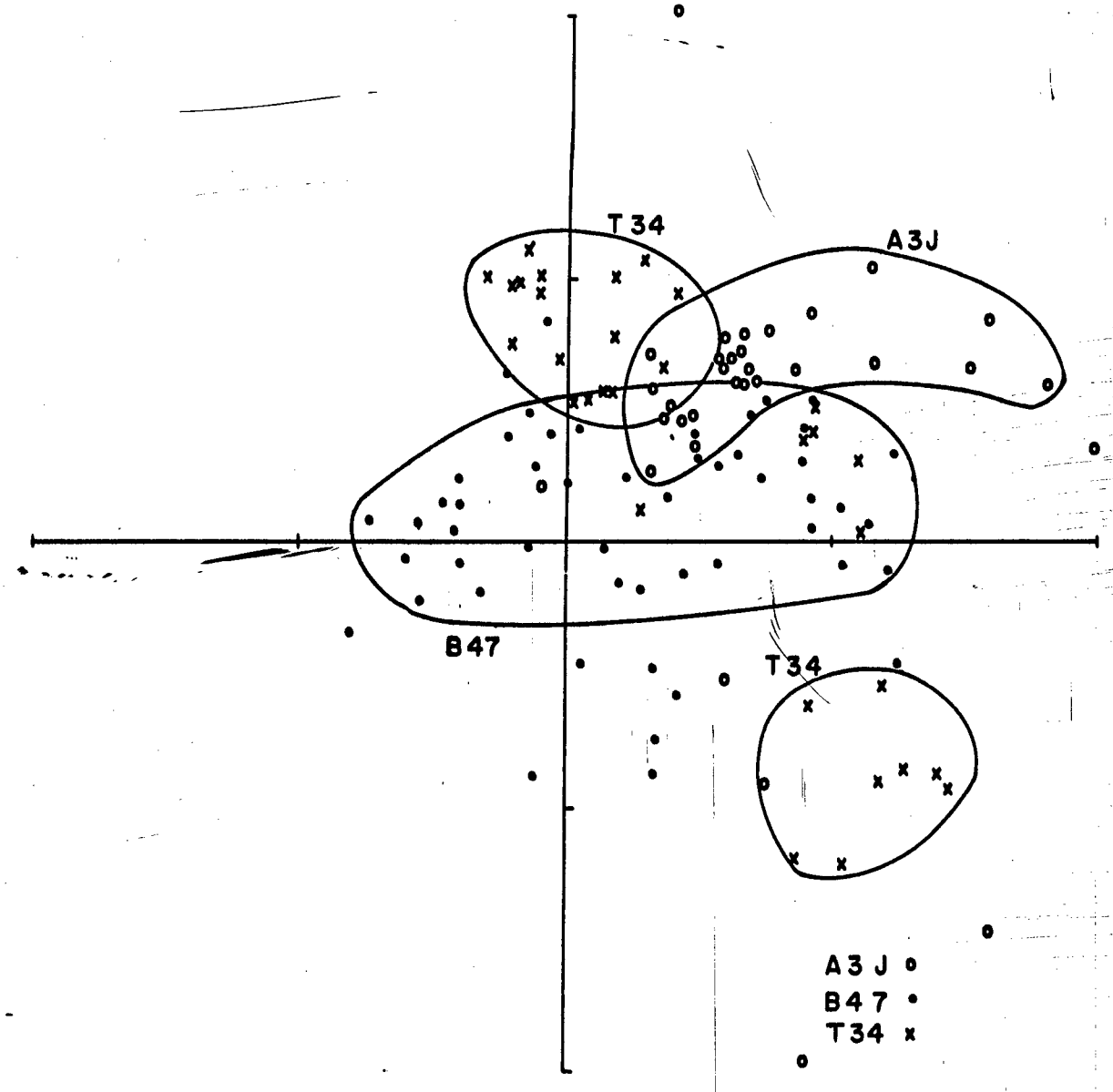

Fig. 19 - Projection of descriptor vectors of three objects upon the plane of the cosine and sine coefficients of the fifth harmonic. Descriptor vectors satisfy Eq. (21). The appearance of two distinct clusters for the T34 tank is attributed to the significant difference between those views in which the tank's gun is visible and those in which it is not.

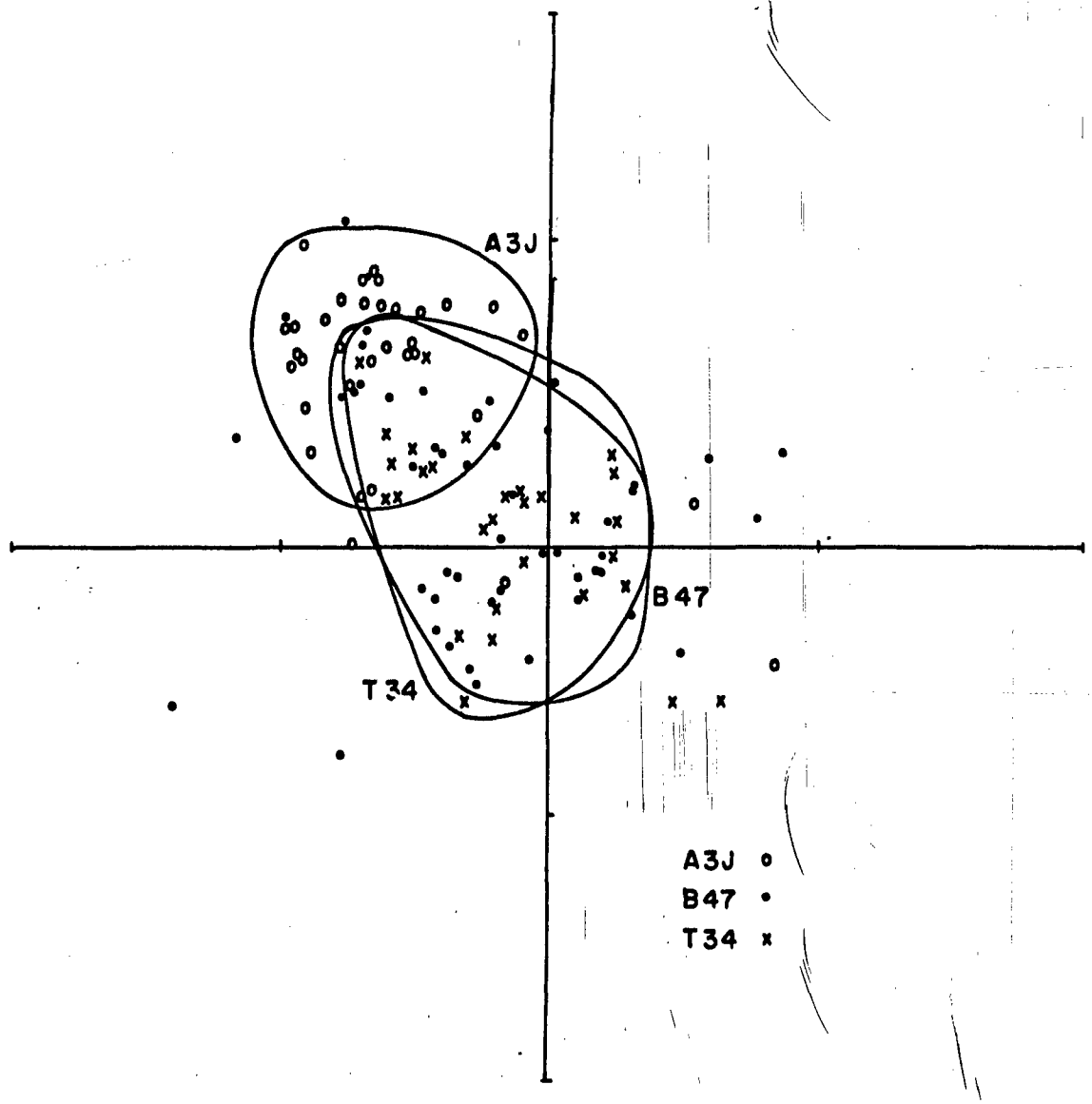

Fig. 20 - Projection of descriptor vectors of three objects upon the plane of the cosine and sine coefficients of the sixth harmonic. Descriptor vectors satisfy Eq. (21).

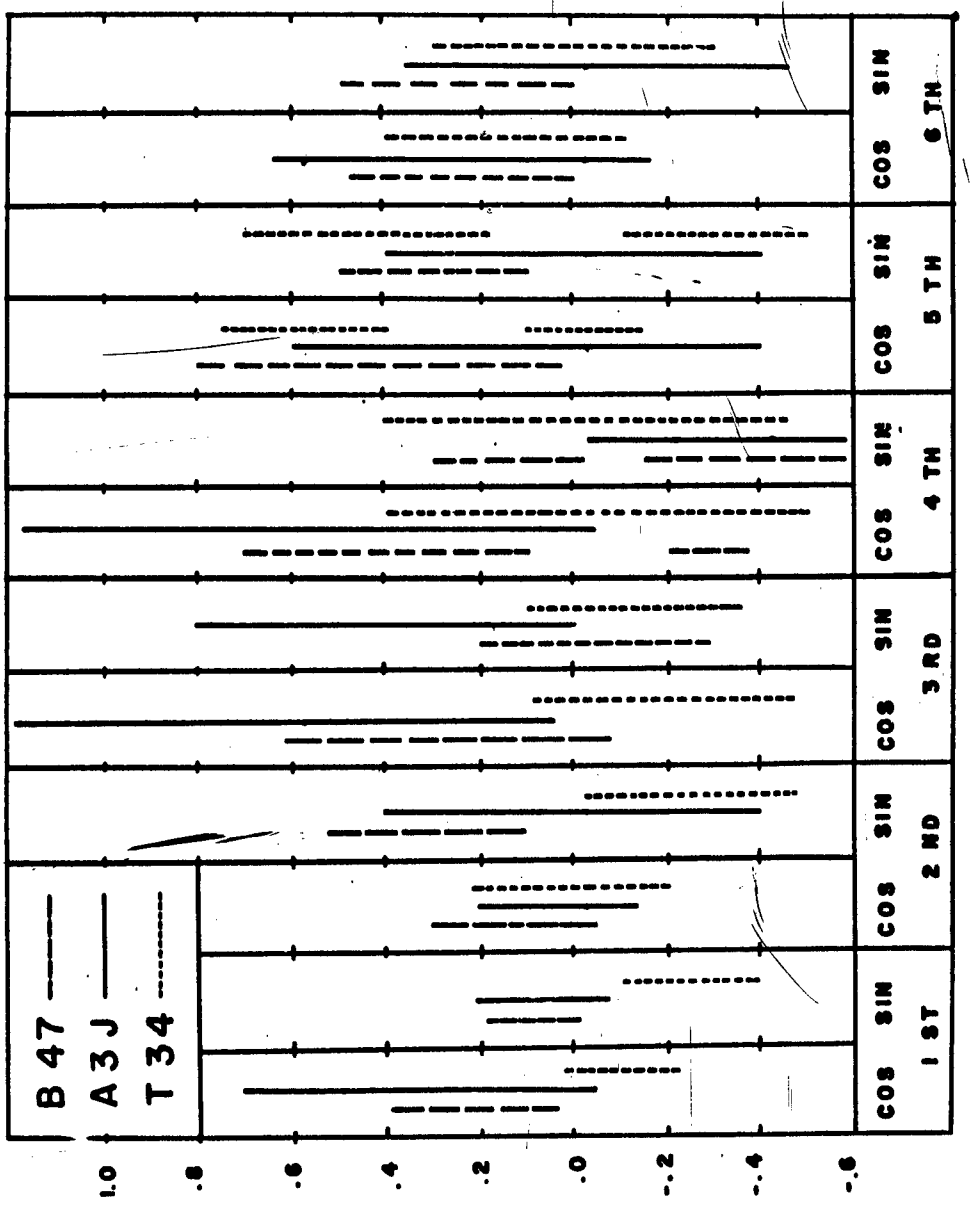

Fig. 21 - Range of individual components of the 12-component descriptor vectors for three objects. The descriptor vectors have been adjusted to satisfy Eq. (21).

The present report deals with descriptor vectors the components of which are the cosine and sine coefficients of the Fourier series expansion of the $\phi(\ell)$ curve of a given figure. It is clear that is is easier to formulate a measure of similarity for the descriptor vectors than it is to do this for the contours which these descriptors represent. It is also clear that continuous deformation of a contour will lead to continuous change of the $\phi(\ell)$ curve and continuous variation of the Fourier coefficients. Thus the similarity of two figures should manifest itself in the components of the vectors being approximately equal.

There are several standard techniques for classifying patterns on the basis of n-dimensional descriptor vectors of some type. In one, the distance is measured in n-space from the end-point of the descriptor vector derived from a given unidentified figure to the end-points of descriptor vectors derived from a set of standard figures. The unknown is then identified as the character associated with that vector to which this distance is smallest. Various transformations and deformations of the n-dimensional vector space may be carried out to improve the likelihood of correct identification if the statistical properties of the descriptors are known.[8]

Another standard technique involves subdividing the n-dimensional descriptor space into cells or regions. The components of the descriptor vector of an unidentified figure are considered as the coordinates of a point. The unknown character is then identified as belonging to that class in whose region in n-space this point falls.[9]

In general, no direct correspondence can be established between the measure of similarity in terms of the descriptor vectors and the similarity of various features of the character themselves. For the descriptors under consideration here, measures of similarity do exist which have definite physical interpretations both in terms of the vectors in n-space and in terms of the $\phi(\ell)$ contour representation. Consider pairs of vectors in n-space; a plausible measure of similarity is the angle θ between them. The smaller this angle, the more nearly parallel and, in this sense, more nearly similar are the vectors. Now the angle θ_{AB} between two vectors $\vec{A}$ and $\vec{B}$ is given by

$$\theta_{AB} = \cos^{-1} \frac{\vec{A} \cdot \vec{B}}{|\vec{A}||\vec{B}|} . \tag{23}$$

Thus

$$\cos \theta_{AB} = \frac{\sum_{i=1}^{n} A_i B_i}{\left(\sum_{i=1}^{n} A_i^2 \right)^{1/2} \left(\sum_{i=1}^{n} B_i^2 \right)^{1/2}} . \tag{24}$$

If the components of the vectors $\vec{A}$ and $\vec{B}$ are the Fourier coefficients of $\phi(\ell)$ functions derived from two contours, it can be shown that $\cos\theta_{AB}$, the measure of similarity in the descriptor n-space, is the approximate normalized cross-correlation $\rho_{\phi_a\phi_b}(0)$ of the functions $\phi_a(\ell)$ and $\phi_b(\ell)$.

By definition, the cross-correlation

$$R_{\phi_a\phi_b}(\lambda) = E[\phi_a(\ell)\ \phi_b(\ell-\lambda)]. \tag{25}$$

For ϕ_a and ϕ_b periodic with the same period T, Eq. (25) is equivalent to

$$R_{\phi_a\phi_b}(\lambda) = \frac{1}{T}\int_{-T/2}^{T/2} \phi_a(\ell)\ \phi_b(\ell-\lambda)d\ell\ . \tag{26}$$

Now

$$\phi_a(\ell) = \sum_{i=1}^{\infty} A_{2i-1}\cos i\ell + A_{2i}\sin i\ell \tag{27a}$$

and

$$\phi_b(\ell) = \sum_{j=1}^{\infty} B_{2j-1}\cos j\ell + B_{2j}\sin j\ell\ , \tag{27b}$$

since the $\phi(\ell)$ functions have zero mean.

Substituting the expressions for ϕ_a and ϕ_b of Eqs. (27a and b) into Eq. (26), and taking into account that $T = 2\Pi$, one may write

$$R_{\phi_a\phi_b}(0) = \frac{1}{2\Pi}\int_{-\Pi}^{\Pi}\left\{\sum_{i=1}^{\infty}\sum_{j=1}^{\infty}(A_{2i-1}\cos i\ell + A_{2i}\sin i\ell)\right. \tag{28}$$

$$\left.\times\ (B_{2j-1}\cos j\ell + B_{2j}\sin j\ell)\right\}\ d\ell\ .$$

Carrying out the indicated multiplication and interchanging the order of summation and integration, one obtains

$$R_{\phi_a\phi_b}(0) = \sum_{i=1}^{\infty}\sum_{j=1}^{\infty}(A_{2i-1}B_{2j-1})\frac{1}{2\pi}\int_{-\pi}^{\pi}\cos i\ell\cos j\ell\,d\ell$$

$$+ (A_{2i}B_{2j})\frac{1}{2\pi}\int_{-\pi}^{\pi}\sin i\ell\sin j\ell\,d\ell$$

(29)

$$+ (A_{2i-1}B_{2j})\frac{1}{2\pi}\int_{-\pi}^{\pi}\cos i\ell\sin j\ell\,d\ell$$

$$+ (A_{2i}B_{2j-1})\frac{1}{2\pi}\int_{-\pi}^{\pi}\sin i\ell\cos j\ell\,d\ell.$$

Taking into account that

(30a) $$\frac{1}{\pi}\int_{-\pi}^{\pi}\cos i\ell\cos j\ell\,d\ell = \delta_{ij}\ ,$$

(30b) $$\frac{1}{\pi}\int_{-\pi}^{\pi}\sin i\ell\sin j\ell\,d\ell = \delta_{ij}\ ,\ \text{and}$$

(30c) $$\frac{1}{\pi}\int_{-\pi}^{\pi}\cos i\ell\sin j\ell\,d\ell = 0,$$

one then may obtain

(31) $$R_{\phi_a\phi_b}(0) = \frac{1}{2}\sum_{i=1}^{\infty}\sum_{j=1}^{\infty}(A_{2i-1}B_{2j-1})\delta_{ij} + (A_{2i}B_{2i})\delta_{ij}\ ,$$

which may be rewritten as

(32) $$R_{\phi_a}R_{\phi_b}(0) = \frac{1}{2}\sum_{i=1}^{\infty}A_iB_i\ .$$

The normalized cross-correlation ρ is defined as

(33) $$\rho_{\phi_a\phi_b}(T) = \frac{R_{\phi_a\phi_b}(T)}{R_{\phi_a\phi_a}(0)^{1/2}\,R_{\phi_b\phi_b}(0)^{1/2}}$$

which has the property that

$$\rho_{\phi_a\phi_b}(0) \leq 1, \tag{34}$$

with

$$\rho_{\phi_a\phi_b}(0) = 1; \tag{35}$$

implying that

$$\phi_a(\ell) = C\ \phi_b(\ell), \tag{36}$$

if ϕ_a and ϕ_b are periodic, piecewise continuous functions.[10]

Now, while the Fourier expansion of a $\phi(\ell)$ function in general leads to an infinite series, it has been shown already (Section III) that for practical purposes the function may be adequately represented by a truncated Fourier series of n/2 harmonics, where n is the number of components in the corresponding descriptor vector.

Combining Eqs. (32) and (33), and taking into account that A_i and B_i are zero for $i > n$, one obtains

$$\rho_{\phi_a\phi_b}(0) = \frac{\sum_{i=1}^{n} A_i B_i}{\left(\sum_{i=1}^{n} A_i^2\right)^{1/2}\left(\sum_{i=1}^{n} B_i^2\right)^{1/2}} \tag{37}$$

The expression for $\rho_{\phi_a\phi_b}$ in Eq. (37) in precisely that of Eq. (24) for $\cos\theta_{AB}$. Therefore

$$\rho_{\phi_a\phi_b}(0) = \cos\theta_{AB}. \tag{38}$$

In view of this correspondence, the two previously mentioned bases for classifying figures may be evaluated. Consider first the technique of classifying figures according to the distances between the end points of their descriptor vectors and the end points of the set of standard vectors. With the loss of some information, all the vectors may be reduced to the common length unity by the transformation

(39) $$A' = \frac{A}{|A|} ,$$

which implies that

(40) $$A_i' = \frac{A_i}{\left[\sum_{i=1}^{n} A_i^2\right]^{1/2}}$$

From simple geometrical consideration it is clear that the measure of similarity for this case,

(41) $$d^2 = \sum_{i=1}^{n} (A_i'-B_i')^2 ,$$

is equivalent to the measure $\cos \theta_{AB}$ in the sense that both will give the same ordering.

It is intuitively clear, therefore, that the measure

(42) $$D^2 = \sum_{i=1}^{n} (A_i-B_i)^2$$

is better, since it is based on a more complete description of a given character.

It is, in fact, the mean square difference of the $\phi(\ell)$ functions of the figures associated with $\vec{A}$ and $\vec{B}$. This may be shown by the following: Consider the functions $\phi_a(\ell)$ and $\phi_b(\ell)$ with zero mean and period 2Π. Their mean square difference is

(43) $$E_{MS} = \frac{1}{2\Pi}\int_{-\Pi}^{\Pi} [\phi_a(\ell) - \phi_b(\ell)]^2 d\ell .$$

As before, one may adequately represent $\phi_a(\ell)$ and $\phi_b(\ell)$ by their truncated Fourier series of n/2 harmonics. Then

$$E_{MS} = \frac{1}{2\pi}\int_{-\pi}^{\pi}\left[\sum_{i=1}^{n/2} A_{2i-1}\cos i\ell + A_{2i}\sin i\ell - B_{2i-1}\cos i\ell - B_{2i}\sin i\ell\right]^2 d\ell$$

$$= \frac{1}{2\pi}\int_{-\pi}^{\pi}\left[\sum_{i=1}^{n/2}(A_{2i-1}-B_{2i-1})\cos i\ell + (A_{2i}-B_{2i})\sin i\ell\right]$$

$$\times\left[\sum_{j=1}^{n/2}(A_{2j-1}-B_{2j-1})\cos j\ell + (A_{2j}-B_{2j})\sin j\ell\right]d\ell \qquad (44)$$

$$= \sum_{i=1}^{n/2}\sum_{j=1}^{n/2}(A_{2i-1}-B_{2i-1})(A_{2j-1}-B_{2j-1})\frac{1}{2\pi}\int_{-\pi}^{\pi}\cos i\ell\cos j\ell\, d\ell$$

$$+ (A_{2i-1}-B_{2i-1})(A_{2j}-B_{2j})\frac{1}{2\pi}\int_{-\pi}^{\pi}\cos i\ell\sin j\ell\, d\ell$$

$$+ (A_{2i}-B_{2i})(A_{2j-1}-B_{2j-1})\frac{1}{2\pi}\int_{-\pi}^{\pi}\sin i\ell\cos j\ell\, d\ell$$

$$+ (A_{2i}-B_{2i})(A_{2j}-B_{2j})\frac{1}{2\pi}\int_{-\pi}^{\pi}\sin i\ell\sin j\ell\, d\ell.$$

Taking into account Eqs. (30a, b, c) one may reduce Eq. (44) to

$$E_{MS} = \frac{1}{2}\sum_{i=1}^{n/2}\sum_{j=1}^{n/2}(A_{2i-1}-B_{2i-1})(A_{2j-1}-B_{2j-1})\delta_{ij} + (B_{2i}-B_{2i})(A_{2j}-B_{2j})\delta_{ij}$$

$$= \frac{1}{2}\sum_{i=1}^{n}(A_i-B_i)^2. \qquad (45)$$

Comparing the expression for E_{MS} of Eq. (45) with that for D^2 in Eq. (32), one obtains the equivalence of the criteria

$$\frac{1}{2} D^2 = E_{MS}. \tag{46}$$

In view of Eq. (46), the techniques of improving recognition by distorting the vector space, to expand some components and contract others, can be reinterpreted as filtering of the $\phi(\ell)$ functions.

The second standard technique of character recognition which has been mentioned above involves classifying figures according to the regions of n-space occupied by the end-points of their descriptor vectors. The regions may be defined by hyperplanes separating each pair of different figures in the set of distinct figures expected. The classification operation could be performed upon a given $\phi(\ell)$ function by a device consisting of phase-sensitive detectors to generate the descriptor vectors and a resistance-diode matrix to effect the separation by hyperplanes. It can be shown that the classification scheme based upon this principle will lead to greater likelihood of correct identification than any scheme based upon the measure D^2, even if the descriptor space is linearly distorted in such a manner as to improve the grouping of classes.[9]

So far, relations have been shown between the measures of similarity in vector space and measures of similarity between different $\phi(\ell)$ curves. It remains to be demonstrated that these have relevance to the recognition problem in the sense that figures that appear similar to a human being lead to $\phi(\ell)$ functions that are similar according to criteria that can be formulated mathematically.

The evidence available indicates that the similarity of the figures is in fact reflected in the similarity of the $\phi(\ell)$ curves; this is indicated by several sets of experimental evidence.

First, a series of comparisons was performed on the descriptor vectors of the contours of Fig. 22. The measures of similarity $\cos \theta_{AB}$ and D^2 were computed for each pair of vectors. Part of the resulting table of matches is shown in Fig. 23, where the figures are arranged in order of decreasing similarity. It can be seen that the similarity detected in the vectors does indeed correspond quite well to the similarity that a person looking at the figures might consider reasonable. It should be noted that essentially the same ordering of best matches was given by the criterion $\cos \theta_{AB}$ and the criterion D^2. Furthermore, it was found that adding components to the descriptor vectors beyond the cosine and sine term coefficients of the first three harmonics had no appreciable effect on the ordering.

Second, a total of seven aircraft models and one tank model were photographed from various elevation and azimuth angles and 12-dimensional descriptor vectors were computed for each view. (Besides the A3J and B47, the aircraft included were a DC3, F94C, B70, B58, and Super G Constellation.)

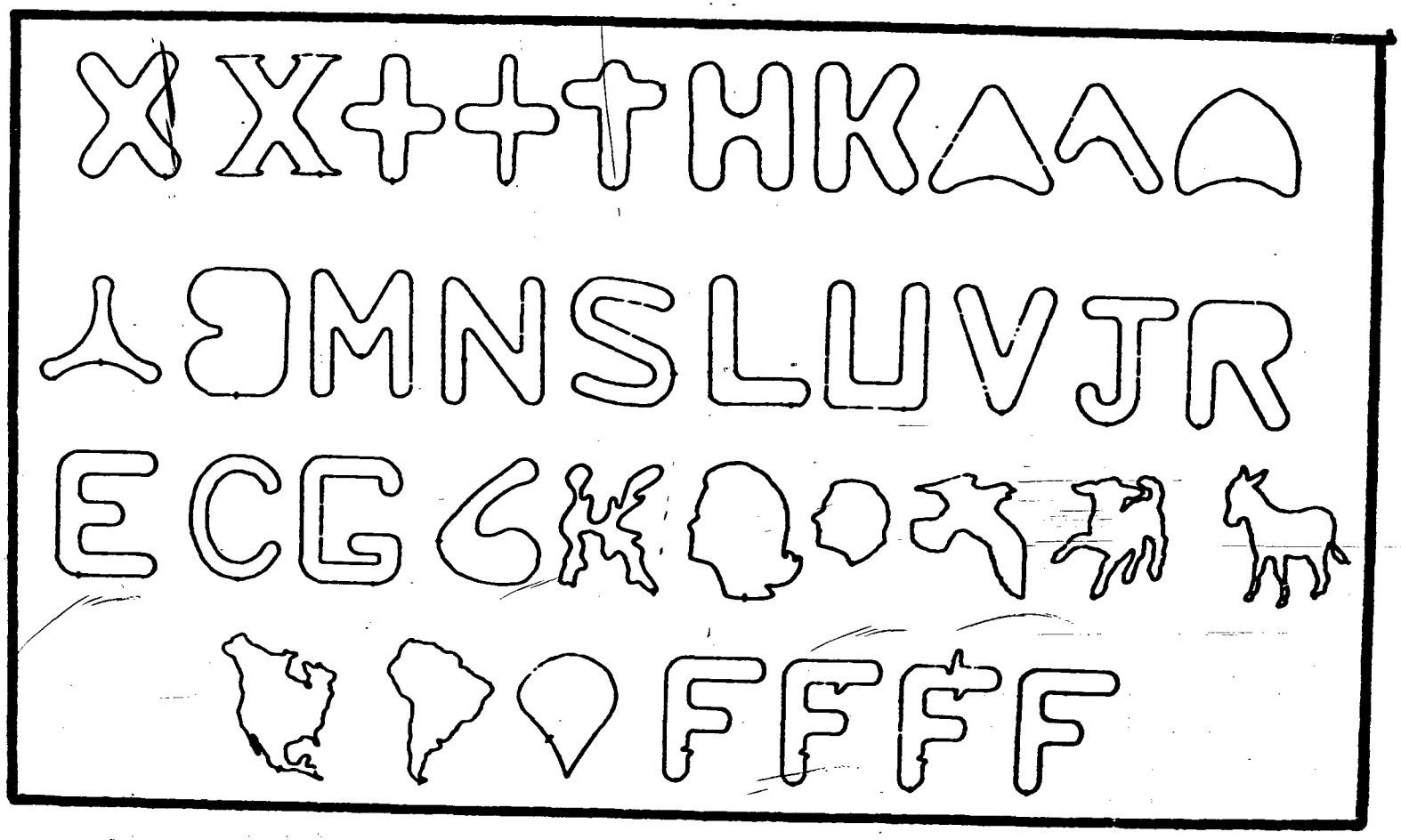

Fig. 22 - A set of contours

Character	Order of matching and cosine of angle				
	0.983	0.968	0.953	0.756	0.722
					
	0.972	0.954	0.766	0.662	0.655
					
	0.977	0.913	0.857	0.750	0.677
					
	0.906	0.768	0.767	0.742	0.722
					
	0.974	0.968	0.966	0.778	0.745
					
	0.962	0.745	0.722	0.722	0.666
					
	0.913	0.887	0.682	0.662	0.657
					

Fig. 23 - Order of matching and cosines of angles between descriptor vectors for selected figures from set shown in Fig. 22.

By looking at projections of the descriptor vectors in 12-space upon various planes (Figs. 14-19), one can see that different views of a given object tend to result in descriptor vectors which fall into clusters, and that clusters caused by different objects tend to be disjointed.

Each components of the descriptor vectors is a continuous and periodic function of the azimuth and elevation angles. From this fact one can deduce that the locus of the descriptor vector end-points, as the azimuth and elevation angles range through all possible values, is a closed surface on which any point can be specified by two parameters. Thus the distribution of the descriptor vectors that is to be expected if descriptors are derived for various views of one given object varies in a significant way from the distribution to be expected if descriptors are derived for a number of similar (but not identical) objects looked at in the same way. The latter set of descriptor vectors could be expected to form a cluster, with points dense near its center and sparsely distributed farther from the center.

This difference is significant for practical purposes when descriptors are to be used for classifying figures. A common way of identifying an unknown vector involves measuring its distance to the mean vector of a sample set of a given class. The unknown is then identified as a member of that class if the distance is sufficiently small. This technique is reasonable only if one expects that the mean vector falls in a region where the sample descriptor vectors are dense. It is not reasonable if the sample descriptor vectors are distributed along a surface that may at every point be quite far from the mean vector.

The difference between the two cases may become clearer if we consider two analogous physical situations that illustrate the difference. In each case, we shall be given the three cartesian coordinates of a point and shall be asked if the point falls inside either of a pair of metal objects fixed in space, which we shall have been allowed to examine and measure previously, but which will no longer be available for a direct test. The first pair of objects will be rather shapeless lumps of solder. Clearly, we will be able to at least make a reasonable guess about the given point if we remember the location of the centers of gravity of the lumps and very roughly their approximate diameters. The second pair of objects will be contorted loops of thin wire. It is clear that a different approach is needed; the centers of gravity of the wires themselves are probably not in the wires, and it may even be that the center of gravity of one wire lies within the other.

Some impression of the shape of distribution of the descriptor vectors may be gained by considering Figs. 24a and b. The figure shows the number of descriptor vectors at a given distance from their means as a function of the distance. The similarity of the curves to Fig. 25c, as compared to Fig. 25d, shows that descriptor vectors do in fact appear to be along surfaces away from their mean.

The separation between groups of descriptors derived from various aircraft viewed from different angles can be judged by considering Fig. 26, which shows projections of the end-points of vectors on a plane chosen to show the maximum separation between their convex hulls. The plane chosen

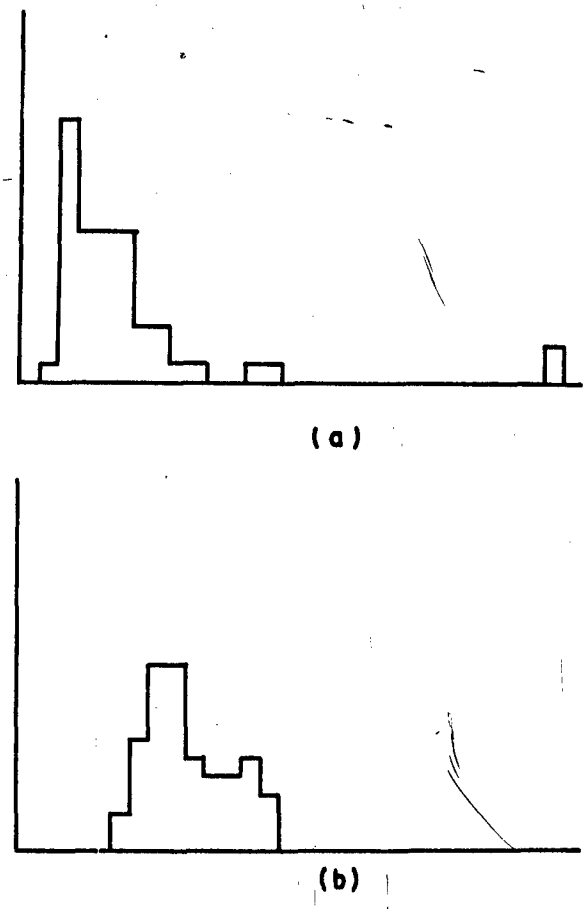

Fig. 24 - Density of descriptor vectors as a function of radial distance from their mean for descriptor vectors of (a) B58 and (b) B70 aircraft.

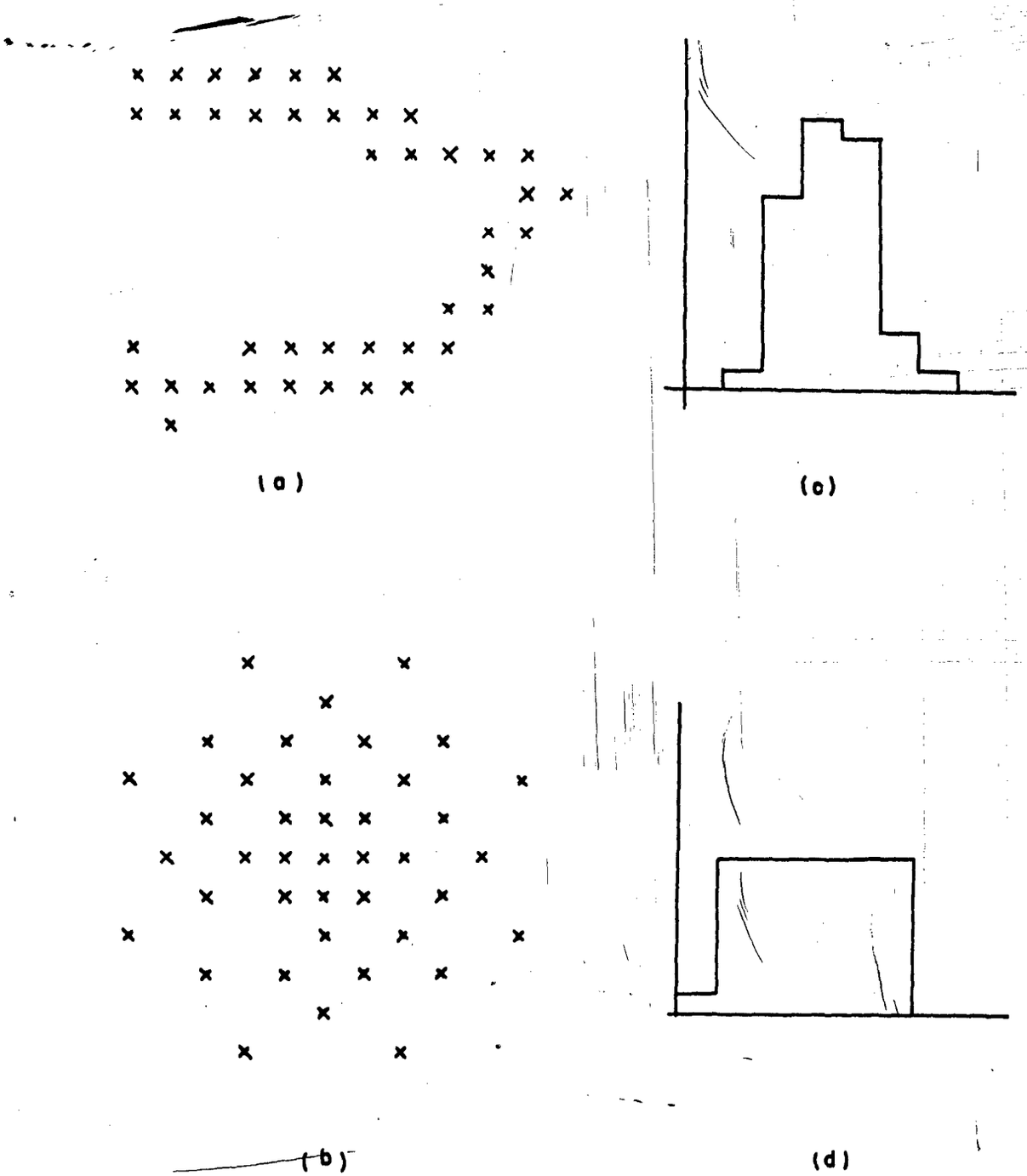

Fig. 25 - Distributions of points in a plane and corresponding curves showing distribution as a function of radial distance from mean. Curve (c) corresponds to distribution (a) and curve (d) to distribution (b).

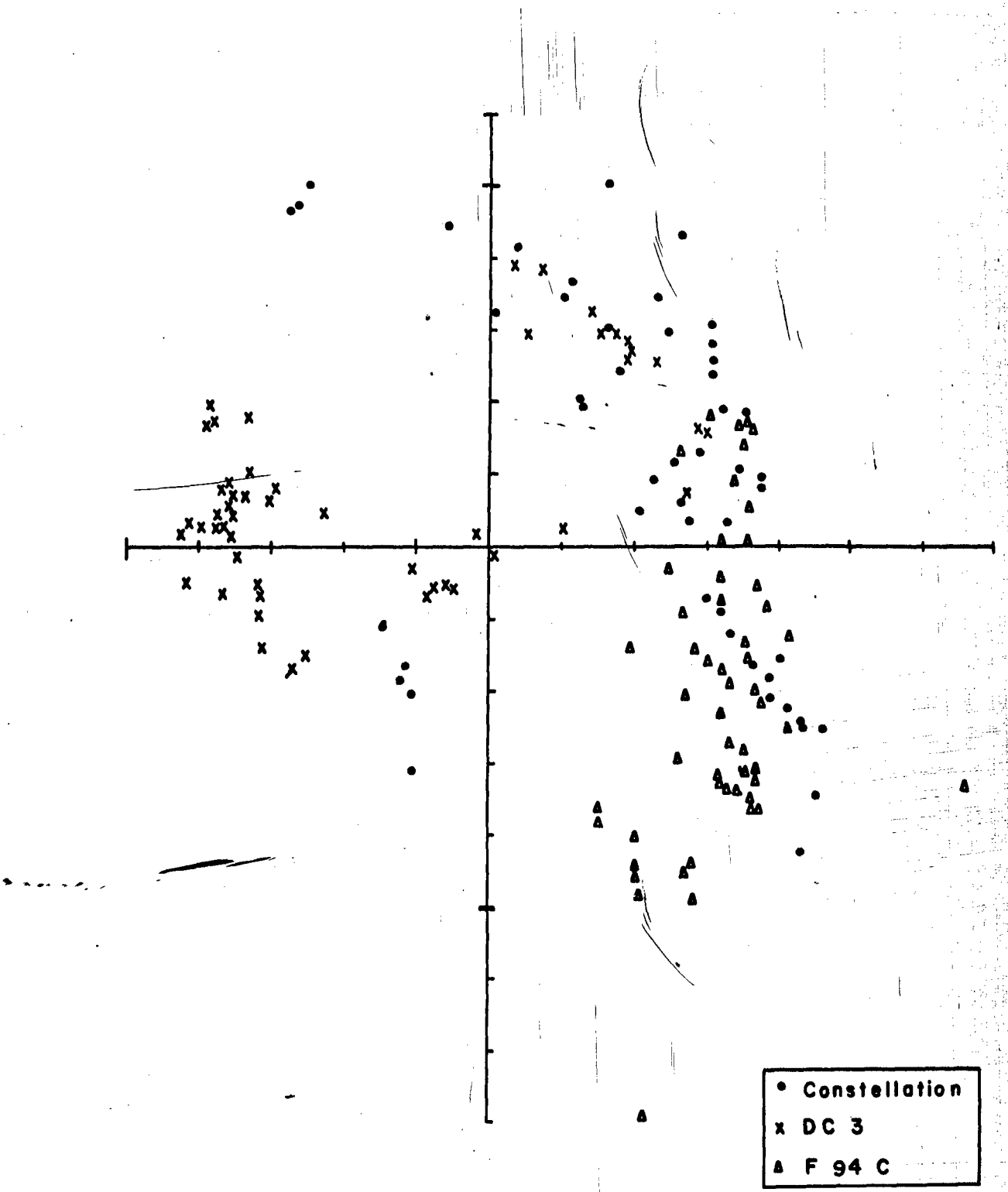

Fig. 26 - Projection of descriptor vectors of three aircraft upon a plane through the means of the classes. This view shows the maximum distances between the classes.

for projecting any three groups was that passing through their centers. It can be seen that more refined techniques are needed for distinguishing between these classes than simple ideas of measuring distances to one reference point for each, or of subdividing the space by hyperplanes.

The most promising approach for solving this problem appears to be to subdivide a class into subclasses, each of which can be effectively characterized by its midpoint. Research in this area remains to be done, even though techniques that separate large groups into suitable subgroups are known.[11]

VI. Alternate Expansions of $\phi(\ell)$ Functions

The process of extracting descriptors for a figure is really a combination of two related but different processes. The first consists of making measurements of some set of physical attributes of the figure. The second is essentially a process of encoding the results of these measurements into a set of numbers. The usefulness of the descriptors obtained ultimately depends on the significance of the attributes that are measured. The coding process, however, is highly important, for it may have a great influence upon how conveniently the resultant descriptor vectors may be categorized. The fundamental attribute of a figure that has been measured throughout the course of the research reported here is the angle between the tangent to its contour and a reference line as a function of distance along the contour. The computation of descriptors by expanding the $\phi(\ell)$ function in Fourier series is only one of many possible encoding process.

It is reasonable to try to express the $\phi(\ell)$ functions as a series of orthogonal functions and to consider the series coefficients to be descriptors. The most familiar series of this type is the Fourier series, the one that has been used so far. In looking for other sets of orthogonal functions that may be useful, one is attracted by functions which assume only the values ± 1. Their obvious merit is their simplicity. It is very easy both to expand an arbitrary function in terms of ± 1 functions analytically and to implement circuitry to do so electronically (Fig. 27). Nevertheless, completely equivalent results can be obtained even more simply.

It will be shown that attempts to obtain descriptor vectors by expanding a $\phi(\ell)$ function in terms of several sets of orthogonal functions whose values are limited to ± 1 can yield results no more useful than those of a much simpler scheme for extracting descriptors.

There are several ways of generating functions having the desired properties. The most instructive begins with a consideration of the properties of Hadamard matrices. A Hadamard matrix of order n is defined as an n x n matrix whose elements assume only the values ± 1 and whose rows and columns are mutually orthogonal. A Hadamard matrix of order 2 is

$$H^{(2)} = \begin{bmatrix} 1 & 1 \\ 1 & -1 \end{bmatrix} \tag{47}$$

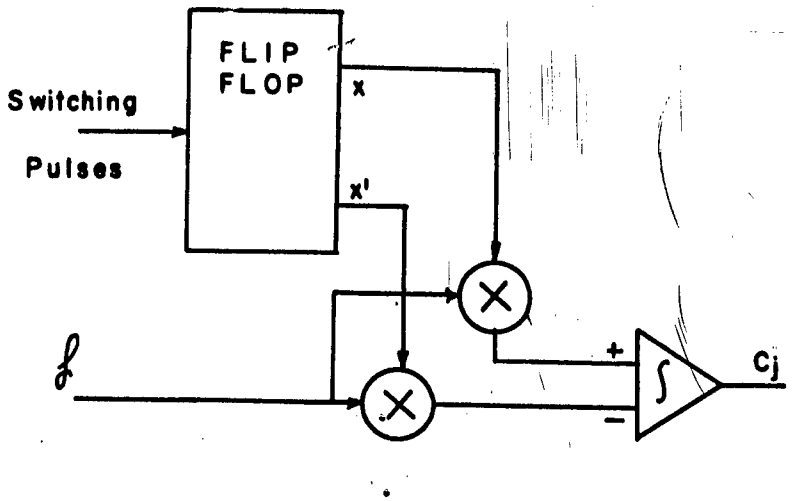

Fig. 27 - Circuit for computing a coefficient of a series expansion of a function f in terms of orthogonal functions assuming the values ± 1.

It can readily be shown that

$$A = \begin{bmatrix} H^{(n)} & H^{(n)} \\ H^{(n)} & -H^{(n)} \end{bmatrix} \tag{48}$$

is a Hadamard matrix of order 2n. Obviously all elements of A have values ± 1. Furthermore, the inner products of each pair of columns of A can be considered as the sum of two inner products of the corresponding columns of the n x n Hadamard matrices. Thus it is clear that

$$\sum_{k=1}^{2n} a_{k,i}\, a_{k,j} \begin{cases} = 0 + 0 = 0 \text{ for } i \neq j \text{ and } i \neq j \pm n \\ = n + n = 2n \text{ for } i = j \\ = n - n = 0 \text{ for } i = j \pm n \end{cases} \tag{49}$$

and the orthogonality relations for the columns are satisfied. A similar proof holds for the rows; thus all requirements for A to be Hadamard are satisfied. Equation (49) allows Hadamard matrices of order 2^m to be generated quite readily.

Orthogonal functions suitable for expanding a function over the interval [0,L] derived from Hadamard matrices of order n are the sets

$$\left\{R_i^{(n)}\right\},\ i = 1,2,\ \text{---}\ n,$$

where a particular function $R_i^{(n)}(x)$ assumes the values of appropriate elements of the $H^{(n)}$ matrix on sections of the interval [0,L]. Specifically

$$R_i^{(n)}(x) = H_{m,i}^{(n)} \qquad \left(\frac{m-1}{n} L \leq x < \frac{m}{n} L\right). \tag{50}$$

As an example, consider the set $\left\{R_i^{(8)}\right\}$. A Hadamard matrix of order 8 is

$$(51) \qquad H^{(8)} = \begin{bmatrix} 1 & 1 & 1 & 1 & 1 & 1 & 1 & 1 \\ 1 & -1 & 1 & -1 & 1 & -1 & 1 & -1 \\ 1 & 1 & -1 & -1 & 1 & 1 & -1 & -1 \\ 1 & -1 & -1 & 1 & 1 & -1 & -1 & 1 \\ 1 & 1 & 1 & 1 & -1 & -1 & -1 & -1 \\ 1 & -1 & 1 & -1 & -1 & 1 & -1 & 1 \\ 1 & 1 & -1 & -1 & -1 & -1 & 1 & 1 \\ 1 & -1 & -1 & 1 & -1 & 1 & 1 & -1 \end{bmatrix}$$

The corresponding set of functions $R_i^{(8)}(x)$ is shown in Fig. 28.

It should be noted that there is no unique Hadamard matrix of order 8. The one considered above was obtained by starting with the $H^{(2)}$ given by Eq. (47) and repeatedly applying Eq. (48). However, any matrix obtained from that of Eq. (51) by any arbitrary reordering of rows and/or columns would still be a Hadamard matrix. Such reordering would, of course, change the order and/or form of the derived functions, R_i.

A given integrable function $f(x)$ may be expanded in terms of $\{R_i^{(n)}\}$ to give a set of n coefficients $\{C_i^{(n)}\}$, where

$$(52) \qquad C_j^{(n)} = \frac{1}{L}\int_0^L f(x)R_j^{(n)}(x)dx.$$

In view of Eq. (50), Eq. (52) may be rewritten as

$$(53) \qquad C_j^{(n)} = \frac{1}{L}\sum_{i=1}^{n} H_{i,j}\int_{\frac{i-1}{n}L}^{\frac{i}{n}L} f(x)dx.$$

But

$$(54) \qquad \int_{\frac{i-1}{n}L}^{\frac{i}{n}L} f(x)dx = \frac{L}{n} f_i(x),$$

where $f_i(x)$ is the average value of $f(x)$ over the ith interval.

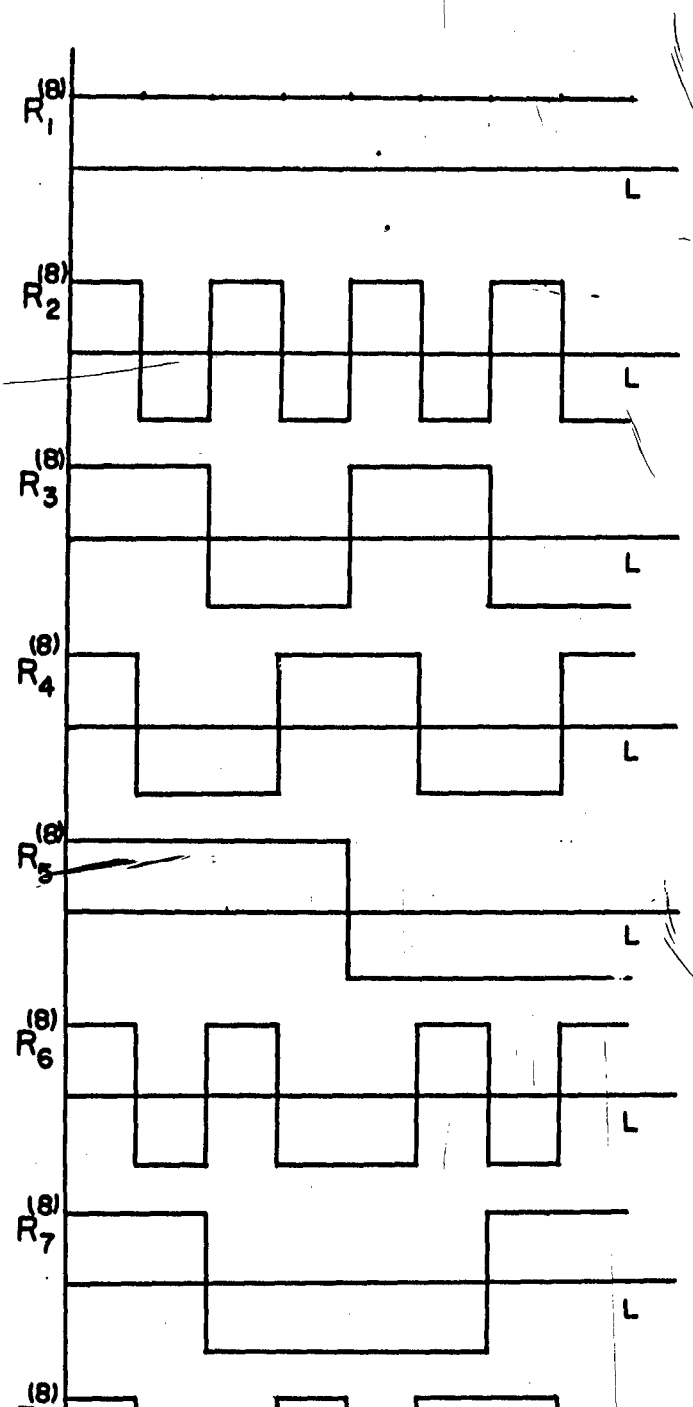

Fig. 28 - A complete set of functions orthogonal on the interval [0,L] and assuming the values ± 1, derived from a Hadamard matrix.

Therefore

$$C_j^{(n)} = \frac{1}{L} \sum_{L=1}^{n} H_{i,j}^{(n)} \frac{L}{n} f_i(x) \tag{55}$$

or

$$C_j^{(n)} = \frac{1}{n} \sum_{i=1}^{n} H_{i,j}^{(n)} f_i(x) . \tag{56}$$

It is clear that all functions $f(x)$ which do not differ in average value over each of the set of n subintervals $\left\{ \left[\frac{i-1}{n} L, \frac{i}{n} L \right], i = 1,2 \text{ --- } n \right\}$, will yield the same set of coefficients $\{C_i^{(n)}\}$. Thus, for the purpose of finding the expansion in terms of the functions $R_i^{(n)}$, a function $f(x)$ is equivalent to the piecewise constant function $F(x)$, with $F(x)$ defined by

$$F(x) = f_i(x), \quad \frac{i-1}{n} L \leq x < \frac{i}{n} L . \tag{57}$$

A given function $F(x)$ can be described completely by specifying a vector $\vec{V}$ of n components such that

$$V_i = F(x) \text{ on } \left[\frac{i-1}{n} L, \frac{i}{n} L \right]. \tag{58}$$

or

$$V_i = f_i(x). \tag{59}$$

Then Eq. (56) may be rewritten as

$$C_j^{(n)} = \frac{1}{n} \sum_{i=1}^{n} H_{i,j}^{(n)} V_i. \tag{60}$$

If $C_j^{(n)}$ is considered as the jth of the n components of the descriptor vector $C^{(n)}$, Eq. (60) is seen to imply the vector equation

$$C^{(n)} = \frac{1}{n}(H^{(n)})^T V. \tag{61}$$

Since $\frac{1}{n} H^{(n)}$ is an orthogonal matrix, Eq. (61) shows that the descriptor vector $\vec{C}^{(n)}$ is the vector $\vec{V}$ rotated by some fixed amount.[13] The descriptor vectors $\vec{C}^{(n)}$ of all figures can be obtained from the corresponding vectors $\vec{V}$ by the same rotation. That means that the vectors $\vec{C}^{(n)}$ derived from a set of different figures will bear exactly the same relationship to each other in n-space as the vectors $\vec{V}$ of the same figures; i.e., the problem of classifying figures on the basis of their descriptor vectors is exactly the same whether the vectors given are of the type $\vec{C}^{(n)}$ or of the type $\vec{V}$.

The orthogonal functions which assume only values ± 1 that have been considered so far have been derived from Hadamard matrices. Alternate ways of generating such functions exist.

Consider first the system of Rademacher functions $\{\Phi_k(x)\}$, defined on the interval [0,1] by

$$\Phi_k(x) = \operatorname{sign}[\sin(2^k \pi x)] \qquad (k = 0,1,2\cdots), \tag{62}$$

where

$$\operatorname{sign} x = \begin{cases} +1 \text{ for } x > 0 \\ 0 \text{ for } x = 0 \\ -1 \text{ for } x < 0 \end{cases} \tag{63}$$

These definitions lead to

$$\Phi_k(x) = \begin{cases} 0 & \text{for } x = \frac{n}{2^k} \\ (-1)^n & \text{for } \frac{n}{2^k} < x < \frac{n+1}{2^k} \end{cases} \tag{64}$$

$$(n = 0,1, \cdots 2^k - 1).$$

The set of Rademacher functions, though orthogonal, is not complete, and therefore not useful for expanding arbitrary functions.[14]

A complete set of orthogonal functions that may be derived from the Rademacher functions is the set of Walsh functions $\{\Psi_k\}$, defined on the interval [0,1] by

$$\Psi_0(x) = 1, \tag{65a}$$

and

$$\Psi_n(x) = \Phi_{n_1+1}(x) \cdot \Phi_{n_2+1}(x) \cdots \Phi_{n_r+1}(x), \tag{65b}$$

for

$$n = 2^{n_1+1} + 2^{n_2+1} + \cdots + 2^{n_r+1}, \tag{65c}$$

with $n_2 > n_2 > \cdots > n_r$, where the $\Phi_i(x)$ are Rademacher functions. The first eight Walsh functions are shown in Fig. 29. Comparison with the functions $\{R_i^{(8)}\}$ derived from the Hadamard matrix of order 8 given in Eq. (51) shows that the two sets of functions are identical, though differently ordered; ($\Psi_0 = R_1^{(8)}$; $\Psi_1 = R_5^{(8)}$; $\Psi_2 = R_3^{(8)}$; $\Psi_3 = R_7^{(8)}$; $\Psi_4 = R_2^{(8)}$; $\Psi_5 = R_6^{(8)}$; $\Psi_6 = R_4^{(8)}$; $\Psi_7 = R_8^{(8)}$).

It is trivial to show that all Walsh functions can be derived from appropriate Hadamard matrices. Consider the Walsh function Ψ_n, with $2^{m-1} \leq n < 2^m$, $m > 1$. It follows from the definition (Eq. (65)) that the highest-order Rademacher function occurring in the product that forms Ψ_n is Φ_m. There are, therefore, exactly 2^m subintervals of [0,1] over which Ψ^n may assume a distinct constant value; Ψ^n may thus be described completely by giving its value on each such subinterval. Let $A_i^{(n)}$ be the value of Ψ_n on the ith such interval, when $1 \leq i \leq 2^m$. There are a total of 2^m Walsh functions Ψ_k which can be described by vectors $\vec{A}^{(k)}$ of 2^m components. Since the Walsh functions are orthogonal on [0,1],

$$\int_0^1 \Psi_n(x)\, \Psi_k(x)\, dx = 0, \quad n \neq k \tag{66}$$

or

$$\sum_{i=1}^{2^m} \int_{\frac{i-1}{2^m}}^{\frac{i}{2^m}} A_i^{(n)} A_i^{(k)} dx = \frac{1}{2^m} \sum_{i=1}^{2^m} A_i^{(n)} A_i^{(k)} = 0. \tag{67}$$

This is equivalent to

$$\vec{A}^{(k)} \cdot \vec{A}^{(n)} = 0, \quad n \neq k. \tag{68}$$

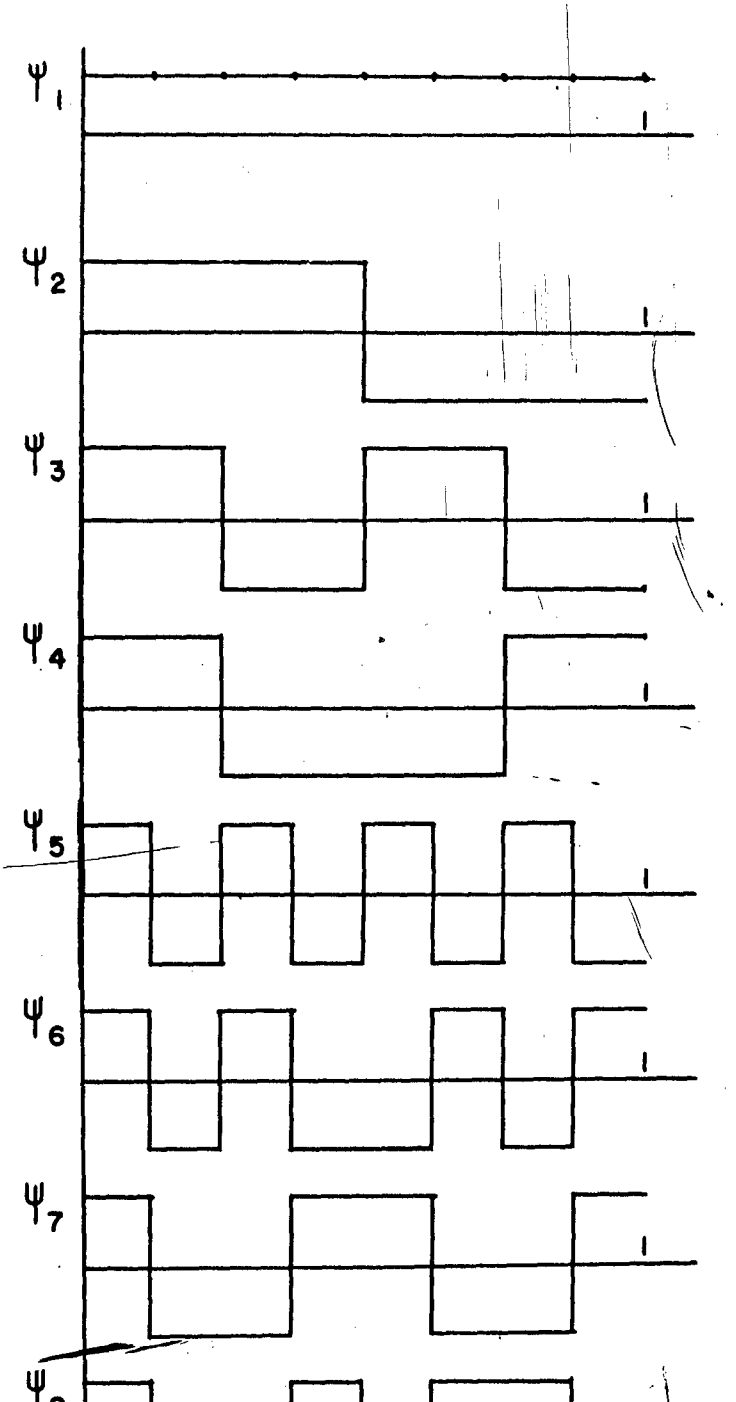

Fig. 29 - The first eight Walsh functions.

If we arrange the 2^m vectors $\vec{A}(j)$ to be the columns of a matrix, it will be Hadamard, and the orthogonal functions $\{R_i^{(2m)}\}$ derived from it will of course be the Walsh functions. It follows that expansion in Walsh functions is no more than a rotation of the simpler descriptor vector $\vec{V}$.

The n-component vector $\vec{V}$ was defined by Eq. (59) to be merely a convenient notation for describing a piecewise constant approximation to a given $\phi(\ell)$ function, with each of its n components assuming the value of the average of the function over one nth of the total interval. It appears that the number of subintervals n must be quite large for the approximation to be satisfactory; i.e., the vector $\vec{V}$ must have many components. It is desirable that a descriptor vector have the minimum number of components consistent with providing an a adequate characterization of the figure. Figure 30 shows the results of attempts to reconstruct a crude silhouette of a B-70 aircraft from a descriptor vector of twelve components. These are the cosine and sine coefficients of the Fourier series expansion of the $\phi(\ell)$ function and from two 12-component vectors of the type $\vec{V}$ derived from the same $\phi(\ell)$ function but assuming different starting points. Comparison of Fig. 30b with Figs. 30c and d shows that on the whole the Fourier series coefficients are roughly equivalent as a set of descriptors to the sets of average values over different subinterval.

However, it is apparent from comparison of Fig. 30c with Fig.30d that the vectors V vary significantly with the starting point on the contour. It was found that the magnitude of the vector difference between the vectors giving rise to Figs. 30c and d was roughly one-third as large as the magnitude of the vectors themselves. This is a very large difference to result from displacing the starting point for tracing the contour only one-twenty-fourth of the total length of the contours (half the length of one subinterval). Descriptor vectors consisting of the coefficients of the Fourier series expansion of the $\phi(\ell)$ function also change with a change in starting point, but it is possible to perform transformations to shift the virtual starting point at will. This is not possible with descriptor vectors of the type $\vec{V}$.

Thus it appears that the descriptor vectors considered throughout most of this report, the coefficients of the Fourier series expansion of the $\phi(\ell)$ function, are, from considerations of conciseness, as good an encoding of the information contained in the $\phi(\ell)$ function as the alternatives so far investigated. Furthermore, they have properties that make it easy to change the virtual origin for the $\phi(\ell)$ function, and to define a standard origin for all figures (see Section IV). However, expansion in Fourier series, though by no means prohibitively complicated, is a process sufficiently involved to make it appear worth while to investigate further what other descriptors might be derived by alternate encoding of the $\phi(\ell)$ functions. The $\phi(\ell)$ function itself appears to be a fundamental and useful description of shape.

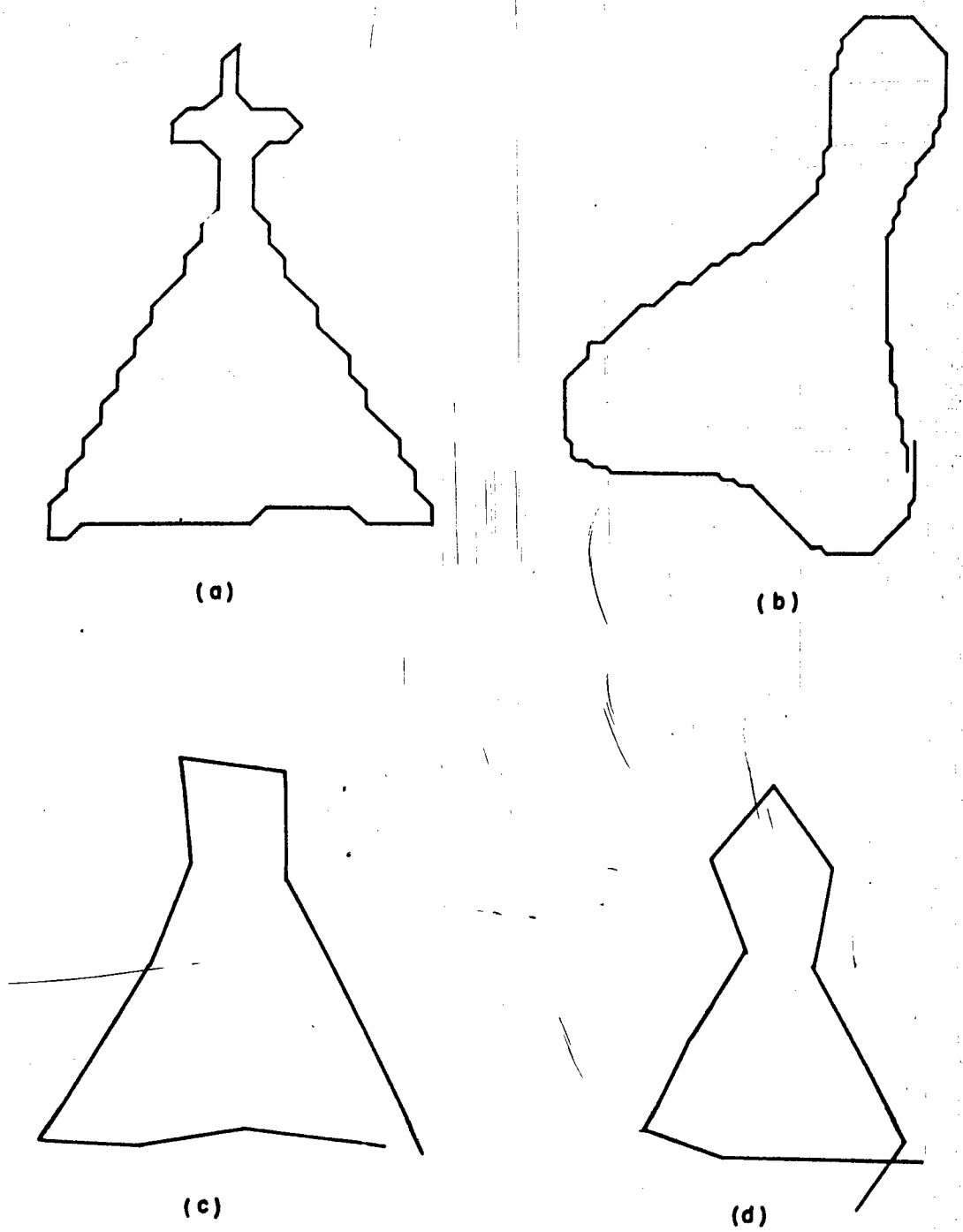

Fig. 30 - An approximate contour representation of a B70 aircraft (a) and reconstructions of the contour from a descriptor vector of twelve components.. Reconstruction (b) is based on the Fourier coefficients of the first 6 harmonics; (c) and (d) are based on descriptor vectors of the type V, defined by Eq. 59, with different starting points on the contour used for calculating the descriptor vectors.

REFERENCES

1. Haagen, W. F., "Video Bandwidth Compression," Report 1222-7, 1 February 1962, Antenna Laboratory, The Ohio State University Research Foundation; prepared under Contract AF 33(616)-7843, Aeronautical Systems Division, Wright-Patterson Air Force Base, Ohio. AD 273 671

2. Raudseps, J. G., "Picture Regeneration from Quantized Data," Report 1222-19, 31 July 1963, Antenna Laboratory, The Ohio State University Research Foundation; prepared under Contract AF 33(616)-7843, Aeronautical Systems Division, Wright-Patterson Air Force Base, Ohio. AD 419 135

3. McConnell, R.L., "Intercontour Redundancy," Master's Thesis, The Ohio State University, 1964.

4. , R. L., "Identification of Shape," Report 820-11, 15 December 1960, Antenna Laboratory, The Ohio State University Research Foundation; prepared under Contract AF 33(616)-5590, Aeronautical Systems Division, Wright-Patterson Air Force Base, Ohio. AD 254 792

5. Fritzsche, D. L., "A Systematic Method for Character Recognition," Report 1222-4, 15 November 1961, Antenna Laboratory, The Ohio State University Research Foundation; prepared under Contract AF 33(616)-7843, Aeronautical Systems Division, Wright-Patterson Air Force Base, Ohio. AD 268 360

6. Final Engineering Report, "Airborne Radar Guidance Techniques," Report 820-12, 31 December 1960, Antenna Laboratory, The Ohio State University Research Foundation; prepared under Contract AF 33(616)-5590, Aeronautical Systems Division, Wright-Patterson Air Force Base, Ohio. Confidential. AD 323 413

7. Marill, T., and Green, D. M., "Statistical Recognition Functions and the Design of Pattern Recognizers," IRE Trans. on Electronic Computers, vol. EC-9, pp. 472-477, December, 1960.

8. Sebestyen, G. S., Decision-making Processes in Pattern Recognition, The Macmillian Company, New York, 1962.

9. Highleyman, W. H., "Linear Decision Functions, with Application to Pattern Recognition," Proc. of the IRE, vol. 50, pp. 1501-1514, June, 1962.

10. Davenport, W. B. Jr., and Root, W. L., An Introduction to the Theory of Random Signals and Noise, McGraw-Hill Book Company, Inc., New York, 1958.

11. Casetti, E., "Classificatory and Regional Analysis by Discriminant Iterations," Technical Reports 11 and 12, Northwestern University; prepared under Contract NONR 1228(26), Office of Naval Research, Geography Branch.

12. Peterson, W. W., Error-correcting Codes, M.I.T. Press, Cambridge, 1962.

13. Stoll, R. R., Linear Algebra and Matrix Theory, McGraw-Hill Book Company, Inc., New York, 1952.

14. Naas, I., and Schmid, H. L., editors, Mathematisches Wörterbuch, Pergamon Press, Oxford, 1962.

DISTRIBUTION LIST
Contract AF33(616)-1267

No. of Copies	
3 (incl 1 repro)	Air Force Avionics Laboratory Attn: AVNT (N. R. Banke) Wright-Patterson AFB, Ohio 45433
1	Research and Technology Division Attn: SEPIR (Library) Wright-Patterson AFB, Ohio 45433
1	Headquarters USAF Director of Research and Technology Attn: AFRSTB (Mr. D. R. McKanna) Washington, D. C. 20330
1	Hq. Research and Technology Division Bolling AFB Attn: RTHR (Mr. W. J. Brown) Washington, D. C. 20332
1	Rome Air Development Center Attn: Documents Library, EMALD Griffiss AFB, New York 13442
1	Research and Technology Division Attn: SEQDD (F. L. Palazzo) Wright-Patterson AFB, Ohio 45433
1	Air Force Cambridge Research Center Attn: Electronic Research Library 230 Albany Street Cambridge 39, Massachusetts
1	Director Air University Library Maxwell AFB, Alabama
1	Ballistic Systems Division AF Unit Post Office Los Angeles, California 90045
1	Rome Air Development Center Attn: L. Sinnamon, Jr., EMIIC Griffiss AFB, New York 13442

DISTRIBUTION LIST
AF33(616)-1267

1	Research and Technology Division Attn: SEPI Wright-Patterson AFB, Ohio 45433
1	Director U. S. Army Electronics Laboratories Hq. U. S. Army Electronics Command Attn: AMSEL-RD-SRE (Mr. S. J. Grossman) Fort Monmouth, New Jersey 07703
1	Commanding General U. S. Army Electronics Command Attn: AMSEL-CB Fort Monmouth, New Jersey 07703
1	Headwuarters, U. S. Liaison Group Project Michigan The University of Michigan Ann Arbor, Michigan
2	Engineering and Development Laboratory Mine Detection Branch Attn: Mr. Chandler Stewart, ERDL Mr. Bernard Schipps Fort Belvoir, Virginia
1	Director U. S. Army Electronics Laboratories Hq. U. S. Army Electronics Command Attn: AMSEL-RD-RDR Fort Monmouth, New Jersey 07703
1	Scientific and Technical Information Facility Attn: NASA Representative (SAK/DL) P. O. Box 5700 Bethesda, Maryland 20014
1	Chief, Bureau of Naval Weapons Department of the Navy Attn: Chief of Electronics Division Washington, D. C. 20360

DISTRIBUTION LIST
AF33(616)-1267

1	Director, Naval Research Laboratory Attn: Code 2021 Washington, D. C. 20390
1	Commanding Officer U. S. Naval Air Development Center Attn: NADC Library Johnsville, Pennsylvania 18974
1	Director, Naval Research Laboratory Attn: Code 5114 Washington, D. C. 20390
1	Massachusetts Institute of Technology Electronics Systems Laboratory Attn: L. Swain, Jr. Cambridge 39, Massachusetts
1	Rand Corporation 1700 Main Street Attn: Dr. H. H. Bailey Santa Monica, California
1	Aerospace Corporation 2400 E. El Segundo Boulevard Attn: Dr. R. W. Rawcliffe El Segundo, California
1	Cornell Aeronautical Laboratory, Inc. 4455 Genesee Street Attn: Dr. R. C. Ziegler Buffalo 21, New York
8	Antenna Laboratory Department of Electrical Engineering The Ohio State University Attn: Dr. R. L. Cosgriff Columbus 10, Ohio
1	University of Michigan Radar Laboratory Attn: A. B. VanderLugt Ann Arbor, Michigan

DISTRIBUTION LIST
AF33(616)-1267

13

Defense Documentation Center
Cameron Station
Attn: TIPDR
Alexandria, Virginia 22314

1

Director
U. S. Army Electronics Laboratories
Hq. U.S. Army Electronics Command
Attn: AMSEL-RD-SSA (Mr. G. Hayes)
Fort Monmouth, New Jersey 07703

Unclassified
Security Classification

DOCUMENT CONTROL DATA - R&D

(Security classification of title, body of abstract and indexing annotation must be entered when the overall report is classified)

1. ORIGINATING ACTIVITY (Corporate author)
The Ohio State University Research Foundation
1314 Kinnear Road, Columbus, Ohio 43212

2a. REPORT SECURITY CLASSIFICATION
Unclassified

2b. GROUP
N/A

3. REPORT TITLE
Some Aspects of the Tangent-Angle vs. Arc Length Representation of Contours

4. DESCRIPTIVE NOTES (Type of report and inclusive dates)
Technical Report - March 1965

5. AUTHOR(S) (Last name, first name, initial)
Raudseps, Juris G.

6. REPORT DATE	7a. TOTAL NO. OF PAGES	7b. NO. OF REFS
March 1965	57	14

8a. CONTRACT OR GRANT NO.	9a. ORIGINATOR'S REPORT NUMBER(S)
AF33(615)-1267 b. PROJECT NO. 414408 c. Task No. 4144 d.	Technical 1801-6 9b. OTHER REPORT NO(S) (Any other numbers that may be assigned this report)

10. AVAILABILITY/LIMITATION NOTICES
Qualified users may obtain copies of this report from Defense Documentation Center. Distribution of this report is restricted in accordance with the US Export Act of 1949 as amended and should not be disseminated to OTS.

11. SUPPLEMENTARY NOTES	12. SPONSORING MILITARY ACTIVITY
	Air Force Avionics Laboratory, Research & Technology Division, AFSC, USAF, Wright-Patterson Air Force Base, Ohio

13. ABSTRACT

A technique is described for characterizing arbitrary, simply connected plane figures by a set of numbers derived from the shape of their outlines. The basis of the description is taken to be the slope of the contour as a function of distance along the contour. This function is expanded in Fourier series, and the series coefficients are taken as a set of descriptors. Topics discussed are the effects of distortion and approximation of contours, reconstruction of figures from their descriptors, and application of the descriptors to pattern recognition. Alternates to the Fourier series expansion of the slope function are also considered.

DD FORM 1 JAN 64 1473

Unclassified
Security Classification

Unclassified
Security Classification

KEY WORDS	LINK A		LINK B		LINK C	
	ROLE	WT	ROLE	WT	ROLE	WT
Pattern recognition Contours Digital computers Orthogonal functions						

INSTRUCTIONS

1. ORIGINATING ACTIVITY: Enter the name and address of the contractor, subcontractor, grantee, Department of Defense activity or other organization *(corporate author)* issuing the report.

2a. REPORT SECURITY CLASSIFICATION: Enter the overall security classification of the report. Indicate whether "Restricted Data" is included. Marking is to be in accordance with appropriate security regulations.

2b. GROUP: Automatic downgrading is specified in DoD Directive 5200.10 and Armed Forces Industrial Manual. Enter the group number. Also, when applicable, show that optional markings have been used for Group 3 and Group 4 as authorized.

3. REPORT TITLE: Enter the complete report title in all capital letters. Titles in all cases should be unclassified. If a meaningful title cannot be selected without classification, show title classification in all capitals in parenthesis immediately following the title.

4. DESCRIPTIVE NOTES: If appropriate, enter the type of report, e.g., interim, progress, summary, annual, or final. Give the inclusive dates when a specific reporting period is covered.

5. AUTHOR(S): Enter the name(s) of author(s) as shown on or in the report. Enter last name, first name, middle initial. If military, show rank and branch of service. The name of the principal author is an absolute minimum requirement.

6. REPORT DATE: Enter the date of the report as day, month, year; or month, year. If more than one date appears on the report, use date of publication.

7a. TOTAL NUMBER OF PAGES: The total page count should follow normal pagination procedures, i.e., enter the number of pages containing information.

7b. NUMBER OF REFERENCES: Enter the total number of references cited in the report.

8a. CONTRACT OR GRANT NUMBER: If appropriate, enter the applicable number of the contract or grant under which the report was written.

8b, 8c, & 8d. PROJECT NUMBER: Enter the appropriate military department identification, such as project number, subproject number, system numbers, task number, etc.

9a. ORIGINATOR'S REPORT NUMBER(S): Enter the official report number by which the document will be identified and controlled by the originating activity. This number must be unique to this report.

9b. OTHER REPORT NUMBER(S): If the report has been assigned any other report numbers *(either by the originator or by the sponsor)*, also enter this number(s).

10. AVAILABILITY/LIMITATION NOTICES: Enter any limitations on further dissemination of the report, other than those imposed by security classification, using standard statements such as:

(1) "Qualified requesters may obtain copies of this report from DDC."

(2) "Foreign announcement and dissemination of this report by DDC is not authorized."

(3) "U. S. Government agencies may obtain copies of this report directly from DDC. Other qualified DDC users shall request through _____."

(4) "U. S. military agencies may obtain copies of this report directly from DDC. Other qualified users shall request through _____."

(5) "All distribution of this report is controlled. Qualified DDC users shall request through _____."

If the report has been furnished to the Office of Technical Services, Department of Commerce, for sale to the public, indicate this fact and enter the price, if known.

11. SUPPLEMENTARY NOTES: Use for additional explanatory notes.

12. SPONSORING MILITARY ACTIVITY: Enter the name of the departmental project office or laboratory sponsoring *(paying for)* the research and development. Include address.

13. ABSTRACT: Enter an abstract giving a brief and factual summary of the document indicative of the report, even though it may also appear elsewhere in the body of the technical report. If additional space is required, a continuation sheet shall be attached.

It is highly desirable that the abstract of classified reports be unclassified. Each paragraph of the abstract shall end with an indication of the military security classification of the information in the paragraph, represented as *(TS)*, *(S)*, *(C)*, or *(U)*.

There is no limitation on the length of the abstract. However, the suggested length is from 150 to 225 words.

14. KEY WORDS: Key words are technically meaningful terms or short phrases that characterize a report and may be used as index entries for cataloging the report. Key words must be selected so that no security classification is required. Identifiers, such as equipment model designation, trade name, military project code name, geographic location, may be used as key words but will be followed by an indication of technical context. The assignment of links, rules, and weights is optional.